

# Early Mesoproterozoic (>1.4 Ga) ages from granulite basement inliers of SE Mexico and their implications on the Oaxaquia concept – Evidence from U-Pb and Lu-Hf isotopes on zircon

Bodo Weber<sup>1,\*</sup> and Carlos H. Schulze<sup>2</sup>

<sup>1</sup>Departamento de Geología, Centro de Investigación Científica y de Educación Superior de Ensenada (CICESE), Carretera Ensenada-Tijuana 3918, Zona Playitas, 22860 Ensenada B.C., Mexico.

<sup>2</sup>Facultad de Ingeniería, Universidad Nacional Autónoma de México (UNAM), Ciudad Universitaria, 04510, México D.F., Mexico.

\* [bweber@cicese.mx](mailto:bweber@cicese.mx)

## ABSTRACT

Four isolated lower crustal complexes also referred to as “Oaxaquia” are exposed in E and SE Mexico. U-Pb zircon dating by laser ablation MC-ICPMS and single-grain Lu-Hf analysis by solution MC-ICPMS were applied to zircon from ortho- and paragneiss samples. Two orthogneiss samples from the Huiznopala Gneiss yield igneous protolith ages of  $1411 \pm 27$  Ma and  $1412 \pm 59$  Ma, respectively. A similar age of  $1444 \pm 16$  Ma was obtained from the “El Catrín” migmatite of the Oaxacan Complex. Hafnium isotope compositions indicate that zircon crystallized from a depleted mantle source with varying amounts of recycled crustal material. The early Mesoproterozoic crust was partially remelted during  $\sim 1.25$  to 1.2 Ga arc magmatism. Paragneisses contain mainly detrital zircon sourced from these  $\sim 1.25$  to 1.2 Ga igneous rocks, indicating the basin received detritus from the arc. None of the Huiznopala and Oaxacan Complex paragneiss samples contained any early Mesoproterozoic or older zircon, which implies an absence of the older protolith material during sedimentation. However, differences in Hf-isotope compositions of some detrital zircons indicate provenances from both typical Oaxaquia (juvenile Mesoproterozoic crust) and more evolved crustal precursors of the same age. Paragneiss from the Guichicovi Complex, instead, contains both early Mesoproterozoic and Paleoproterozoic zircon indicating cratonic sources. The results are interpreted in terms of a “proto-Oaxaquia” oceanic arc system that was active over early Mesoproterozoic times (1.5–1.4 Ga) during the breakup of the Columbia supercontinent. These data further suggest that this arc system was accreted to Amazonia contemporaneously with the  $\sim 1.25$  to 1.2 Ga granitic arc magmatism reported in Oaxaquia and the Eastern Cordillera of Colombia. Stacking of these arc rocks along the continental margin may have caused additional migmatization around 1.1 Ga.

Key words: Oaxaquia; Columbia supercontinent; Rodinia; U-Pb ages; Lu-Hf isotopes; Mexico.

## RESUMEN

En el E y SE de México se encuentran expuestos cuatro complejos de corteza inferior que definen “Oaxaquia”. Se realizó el fechamiento por U-Pb en zircón por ablación láser con MC-ICPMS y análisis

de isótopos de Lu-Hf en granos individuales de zircón en solución por MC-ICPMS en muestras de orto- y paragneis. Dos muestras de ortogneis del Huiznopala arrojaron edades de un protolito ígneo en  $1411 \pm 27$  Ma y  $1412 \pm 59$  Ma, respectivamente. Una edad similar de  $1444 \pm 16$  Ma se obtuvo de la migmatita “El Catrín” del complejo Oaxaqueño. Las composiciones isotópicas de Hf indican que el zircón cristalizó de una fuente en el manto empobrecido con cantidades variadas de corteza reciclada. La corteza del Mesoproterozoico temprano se fundió parcialmente durante un magmatismo de arco entre 1.25 y 1.2 Ga. El paragneis contiene esencialmente zircón detrítico proveniente de estas rocas ígneas con edades de entre 1.25 y 1.2 Ga, indicando que el detritus proviene substancialmente de las rocas de arco. Ninguna de las muestras de paragneis del complejo Oaxaqueño y Huiznopala contiene zircón del Mesoproterozoico temprano o más antiguo, lo que implica ausencia de protolitos más antiguos durante la sedimentación. Sin embargo, las diferencias en la composición isotópica de algunos zircones detríticos indican proveniencias de dos fuentes, uno de Oaxaquia típico (corteza mesoproterozoica juvenil) y un precursor cortical más evolucionado de la misma edad. El paragneis del complejo Guichicovi, en cambio, también contiene zircones del Mesoproterozoico temprano y del Paleoproterozoico, lo que indica fuentes cratónicas. Los resultados se interpretan en términos de un sistema de arco oceánico llamado “proto-Oaxaquia”, que estuvo activo en el Mesoproterozoico temprano (1.5–1.4 Ga) durante la desintegración del supercontinente Columbia. Adicionalmente, los datos sugieren que este sistema de arco fue acrecionado a Amazonia contemporáneamente al magmatismo de arco entre 1.25 a 1.2 Ga, reportado en Oaxaquia y en la Cordillera del Este de Colombia. El apilamiento de estas rocas de arco a lo largo del margen continental pudo haber causado una migmatización de alrededor de 1.1 Ga.

Palabras clave: Oaxaquia; supercontinente Columbia; Rodinia; edades U-Pb; isótopos Lu-Hf; México.

## INTRODUCTION: THE GEOCHRONOLOGY OF THE OAXAQUIA MICROCONTINENT – FROM THE EARLY WORKS TO THE PRESENT

The first attempts to date rocks and minerals in Mexico, more than 50 years ago, were made on either zircon with the Pb- $\alpha$  method or mica with the K-Ar and Rb-Sr methods, mainly from Mesoproterozoic

basement rocks of the Oaxacan Complex (Fries and Rincón-Orta, 1965; Fries and Schmitter, 1962; Fries, 1962a, 1962b; Fries *et al.*, 1966). In these pioneering works huge amounts of zircon per sample were needed to obtain measurable  $\alpha$  activities. Additionally, it was impossible to detect secondary Pb-loss and the presence of initial Pb or inheritance by the Pb- $\alpha$  method. However, the first Pb- $\alpha$  zircon age of  $1110 \pm 125$  Ma (Fries and Schmitter, 1962) agrees astonishingly well with the range of ages obtained by more sophisticated methods on samples of the Oaxacan Complex and related Grenvillian basement exposures of Mexico. In these early works, K-Ar ages of phlogopite and biotite from pegmatites of the Oaxacan Complex ranging from  $940 \pm 40$  Ma to  $855 \pm 30$  Ma (Fries and Rincón-Orta, 1965; Fries and

Schmitter, 1962) are within errors identical to modern and more precise  $^{40}\text{Ar}/^{39}\text{Ar}$  analyses of phlogopite and biotite of  $945 \pm 10$  Ma and  $856 \pm 10$  Ma published forty years later (Keppie *et al.*, 2004).

The differences in mica ages depend on the local or regional cooling histories and mineral size, whereas the U-Pb system in zircon often stays isotopically closed after crystallization due to having closure temperatures as high as  $900^\circ\text{C}$  (Lee *et al.*, 1997) or, in dry granulite facies conditions, even higher ( $950^\circ\text{C}$ , Möller *et al.*, 2002). Classic U-Pb geochronology on zircon using isotope dilution and thermal ionization mass spectrometry (ID-TIMS) was performed by several authors on rocks from the Oaxacan Complex (Keppie *et al.*, 2003, 2001; Schulze, 2011; Solari *et al.*, 2003) and other late Mesoproterozoic (Grenville)

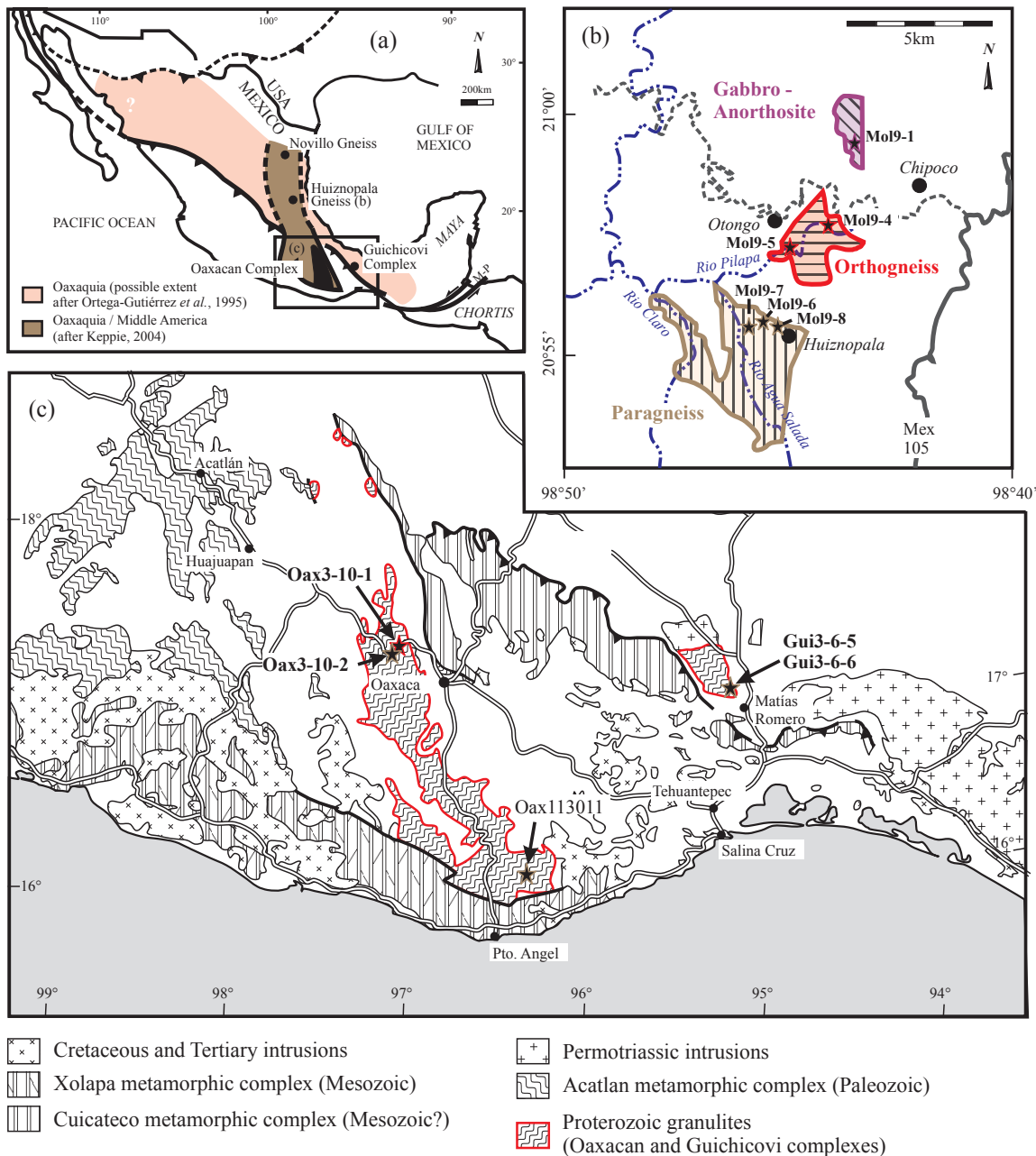


Figure 1. (a) Sketch map showing the proposed extension of the Oaxaquia microcontinent and the four principal exposures of Mesoproterozoic granulite facies rocks in eastern and southern Mexico; (b) major exposures of the Huiznopala Gneiss (adopted from Lawlor *et al.*, 1999) and sample locations; (c) simplified geologic map of crystalline rocks from southern Mexico (Ortega-Gutiérrez *et al.*, 1992) showing sample locations.

exposures in Mexico (Figure 1a) like the Huiznopala Gneiss (Lawlor *et al.*, 1999), the Novillo Gneiss (Cameron *et al.*, 2004), and the Guichicovi Complex (Ruiz *et al.*, 1999; Weber and Köhler, 1999) altogether referred to as the Oaxaquia microcontinent that form the backbone of central, eastern and southern Mexico (Figure 1a; Ortega-Gutiérrez *et al.*, 1995).

Most of the individual zircon fractions analyzed in these studies yielded almost concordant or slightly discordant U-Pb ages in the range from ~1250 to ~970 Ma and, consequently, upper and lower concordia intercept ages were calculated to constrain both protolith crystallization and high-grade metamorphism ages, suggesting arc magmatism at about 1250–1200 Ma and peak granulite facies metamorphism at ~990–970 Ma (Lawlor *et al.*, 1999; Solari *et al.*, 2003; Weber and Köhler, 1999). However, upper intercept ages or even concordant zircon fractions often gave ages in-between the abovementioned values like  $1134 \pm 54$  Ma (upper concordia intercept) or  $1117 \pm 4$  Ma (concordant abraded single grain) both reported from a granitic gneiss of the southern Oaxacan Complex (Keppie *et al.*, 2001). Similar results were obtained from metaigneous rocks of the northern Oaxacan Complex (Keppie *et al.*, 2003) and from a migmatite (El Catrín, Solari *et al.*, 2003) of the same area. The latter yielded an  $1106 \pm 6$  Ma  $^{207}\text{Pb}/^{206}\text{Pb}$  age from a concordant grain that was interpreted to reflect the time of anatexis during an “Olmecan” event (Solari *et al.*, 2003). Furthermore anorthosite-mangerite-charnockite-granite suites (AMCG) intruded the lower crust of Oaxaquia prior to peak metamorphism at *ca.* 1020–1000 Ma (Cameron *et al.*, 2004; Keppie *et al.*, 2003; Schulze, 2011; Solari *et al.*, 2003).

Obviously, the discordia concept using classic ID-TIMS zircon geochronology and concordia intercept ages is limited to two geologic events, either (1) igneous zircon plus metamorphic overgrowth or ancient lead loss or (2) igneous zircon plus inherited zircon core. If additional tectonothermal events occurred, then mixed concordant ages and concordia intercepts with no geologic significance are the consequence. Furthermore, if the geologic events all happened within a relatively short time interval (with respect to the age of the rock), then zircons with several growth phases and inheritance can lead to U-Pb isotope compositions that yield within errors concordant ages without geologic significance (see Weber *et al.*, 2010, for examples). To overcome these problems more sophisticated methods with microanalytical age determination of zircon growth zones are necessary like SHRIMP (Sensitive High Resolution Ion Microprobe) or LA-MC-ICPMS (Laser Ablation Multicollector Inductively Coupled Mass Spectrometry). Detailed laser ablation zircon geochronology using a 10  $\mu\text{m}$  spot size and cathodoluminescence (CL) imaging has shown that zircons from granulite facies migmatites from the southern Oaxacan Complex have average igneous core ages of *ca.* 1.22 Ga (Weber *et al.*, 2010). These cores are rimmed by zircon that grew during migmatization probably some time between 1.10 and 1.05 Ga followed by granulite facies metamorphism producing zircon overgrowths. Metaigneous rocks of the AMCG suite suggest melting of the lower crust about 10–30 Ma prior to granulite facies metamorphism at ~990 Ma (Weber *et al.*, 2010). In the previous works on Oaxaquia inherited zircon cores that are older than ~1.3 to 1.25 Ga are rare and led to the hypothesis that Oaxaquia evolved as a former juvenile arc without significant contamination from older continental crust (Keppie and Ortega-Gutiérrez, 2010; Keppie *et al.*, 2003; Weber and Hecht, 2003). The geologic histories seem to be similar in most of the Mexican granulite exposures (1) a 1.3–1.2 Ga magmatic arc, (2) localized migmatization of the arc rocks, (3) intrusion of AMCG suits at 1.02–1.00 Ga, (4) granulite facies metamorphism at 990–970 Ma, followed by (5) uplift cooling and locally retrogression by hydration reactions of the dry granulite facies assemblages.

Hafnium isotopic composition of zircon and whole rock samples (Weber *et al.*, 2010) support common crustal growth in Mesoproterozoic

times from a depleted mantle source without significant contamination from older continental crust for most of Oaxaquia with one exception – the Huiznopala Gneiss. Previous work on zircons from a garnet-bearing orthogneiss sample of the Huiznopala Gneiss (Weber *et al.*, 2010) yielded significantly lower Hf isotopic ratios and older depleted mantle Hf model ages ( $\text{TDM}_{(\text{Hf})}$ ) compared to all other samples from Oaxaquia (1.8–1.7 Ga vs. 1.6–1.5 Ga). This sample was also the only one in which a >1.5 Ga zircon core was detected. These results led to the distinction between “typical Oaxaquia” oceanic arc-terrane and the contrasting Huiznopala Gneiss that displays considerable amount of contamination from older continental crust (Weber *et al.*, 2010). It was suggested that the Huiznopala Gneiss was emplaced above the Oaxaquia arc terrane at some point during the Grenville orogeny and Rodinia assemblage (Weber *et al.*, 2010). Evidence for early mid-Proterozoic crust in Oaxaquia is known from the “El Catrín” migmatite of the northern Oaxacan Complex. Discordant zircon from this migmatite yielded upper concordia intercept ages of ~1.4 Ga (ID-TIMS; Solari *et al.*, 2003) similar to upper concordia intercept ages reported from the southern Oaxacan Complex (ID-TIMS; Schulze, 2011).

In this contribution U-Pb dating by laser ablation MC-ICPMS was combined with single-grain Lu-Hf isotope analyses by solution MC-ICPMS of zircon. The objectives of this study are (1) to better constrain the previously reported early Mesoproterozoic age of one single zircon grain from the Huiznopala Gneiss, (2) to compare the results with data from the El Catrín migmatite (Northern Oaxaca Complex) and (3) to elucidate the role of early Mesoproterozoic continental influence in (a) metaigneous rocks and (b) detrital zircon from metasedimentary rocks. To meet these objectives, zircons from three metaigneous samples of the Huiznopala Gneiss and one from the El Catrín migmatite were analyzed. The data are complemented by zircon analyses from paragneiss samples from the Huiznopala Gneiss, the Oaxacan Complex and the Guichicovi Complex.

## GEOLOGIC OVERVIEW AND SAMPLE DESCRIPTION

### The Huiznopala Gneiss

In the state of Hidalgo, granulite facies metamorphic rocks were first described by Kuegelgen, 1958) in the central part of the Huayacocotla anticlinorium of the Sierra Madre Oriental. Fries and Rincón-Orta (1965) formally defined the Huiznopala Gneiss and regional mapping of Ochoa-Camarillo (1996) established a total of six separate basement exposures that are covered by Permian and Early Jurassic sedimentary and volcanic rocks. Lawlor *et al.* (1999) performed an integrated work on the Huiznopala Gneiss, including structure, geochemistry, U-Pb zircon geochronology (ID-TIMS), common lead isotopes and thermobarometry, suggesting active arc magmatism from 1.2 to 1.15 Ga followed by ductile deformation and granulite facies metamorphism at ~1.0 Ga with pressure and temperature conditions calculated at ~7.2 kbar and ~725 °C (Lawlor *et al.*, 1999). The authors further noticed that anhydrous granulite facies assemblages were overprinted by at least two retrograde events. Cooling of the Huiznopala Gneiss is constrained by garnet-whole rock ages between ~967 and ~902 Ma with the Lu-Hf method (Scherer *et al.*, 2000) and between ~937 and ~888 Ma with the Sm-Nd method (Patchett and Ruiz, 1987; Scherer *et al.*, 2000). A biotite-whole rock age of  $827 \pm 8$  Ma documents the time of uplift and cooling below the biotite closure temperature (Patchett and Ruiz, 1987).

The three largest exposures, each of which is characterized by typical lithologies, are shown in Figure 1b. (1) West and south of the village of Huiznopala paragneisses were mapped (Ochoa-Camarillo, 1996) which include banded feldspathic paragneiss, calcsilicate gneisses,

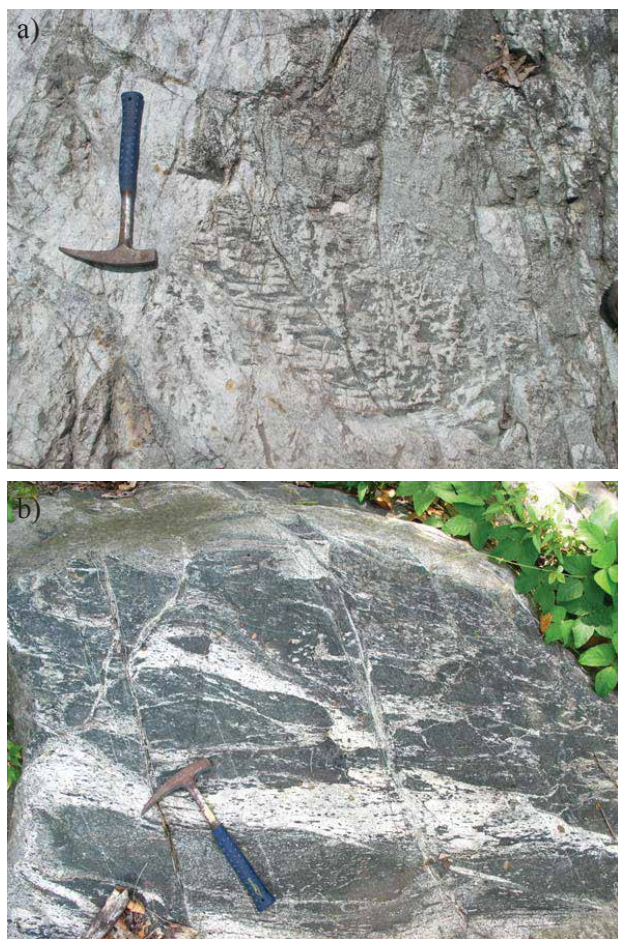


Figure 2. Field photographs of (a) anorthosite with patchy gabbroic inclusions from where sample Mol9-1 was taken; (b) outcrop with anatectic dioritic orthogneiss. Sample Mol9-4 is from the dark paleosome.

and clinopyroxene-rich marbles (Lawlor *et al.*, 1999), in this paper referred to as the “Huiznopala Supracrustal Unit”. Its metasedimentary origin is inferred from 1–2 m thick strata, which are banded on millimeter to centimeter scale (Lawlor *et al.*, 1999), abundant biotite-rich layers, and intercalated calcsilicate rocks and marbles. However, a volcanosedimentary origin of some of the gneisses from the Huiznopala Supracrustal Unit cannot be excluded. (2) Along the Pilapa River, southeast of Otongo (Figure 1b), a sequence of metagneous rocks mainly composed of metatonalite and charnockite, define the Main Series (Lawlor *et al.*, 1999). (3) Meta-anorthosites and associated gabbroic gneisses crop out northwest of the village of Chipoco. The remaining three exposures are of minor dimensions and located between five and 25 km east and southeast of the map area of Figure 1b. They contain orthogneisses of the Main Series (Lawlor *et al.*, 1999).

For this study six samples from the Huiznopala Gneiss were analyzed, which are described briefly in the following section. The sample locations are shown in Figure 1b.

Mol9-1 is a dark (gabbroic) variety from the gabbro-anorthosite sequence NW of Chipoco (20°59'23"N, 98°43'30"W). This rock-type occurs as m-wide patches within the anorthosite (Figure 2a) and appears to represent gabbroic lower crust enclaves. The hosting rock consists almost entirely of equigranular medium-grained plagioclase (andesine). Minor components are orthopyroxene, brown amphibole,

and ilmenite. Biotite is observed in contact with opaque crystals. Most of the orthopyroxene is retrogressed to chlorite. Euhedral apatite and zircon are accessories minerals.

Mol9-4 is a migmatite with banded leucosome and dark grey paleosome (Figure 2b) from the Main Series east of Otongo along the Pilapa River (20°57'39"N, 98°44'08"W). The sample is a granulite from the paleosome and contains partly sericitized plagioclase, clinopyroxene, orthopyroxene and quartz as main mineral phases. Accessories phases are titanite, apatite, zircon and opaque minerals.

Mol9-5 is a garnet-bearing charnockite from the Main Series (orthogneiss) that outcrops SE of Otongo close to the Pilapa River (20°57'09"N, 98°45'00"W, Figure 1b). It is mainly composed of plagioclase, K-feldspar and quartz, having an equigranular hypidiomorphic texture. Minor mineral components are orthopyroxene (bastitized), small (<1mm) garnet, apatite and rutile; the latter partly reacted to titanite.

Mol9-6, Mol9-7, and Mol9-8 are from the paragneiss type locality (Huiznopala Supracrustal Unit) west of the village of Huiznopala along the descent to the Agua Salada River (Figure 1b, Lawlor *et al.*, 1999). Mol9-6 (20°55'46"N, 98°45'31"W) contains abundant mm-sized laths of reddish-brown, partly bleached biotite. Besides biotite, major components are perthitic K-feldspar, plagioclase, quartz and minor mostly bastitized orthopyroxene. The rock has an almost equigranular texture without a defined foliation at microscopic scale. Accessories minerals are apatite, zircon and opaques. Secondary carbonate and sericite occur on fractures.

Mol9-7 (20°55'40"N, 98°45'46"W) is a garnet-rich variety of paragneiss and contains mainly quartz, micro- and mesoperthitic K-feldspar, antiperthitic plagioclase, garnet and minor, partially bastitized orthopyroxene. Euhedral apatite is relatively abundant. Skeletal ilmenite crystals partly reacted to titanite. Chloritized biotite occurs as accessory phase together with zircon and minor tourmaline.

Mol9-8 is a granoblastic felsic granulite composed of microperthitic K-feldspar, quartz, plagioclase and secondary carbonate mixed with opaque minerals forming pseudomorphs, probably after orthopyroxene. Ilmenite crystals partly reacted to titanite. Apatite is an abundant accessory mineral as well as zircon.

### The Oaxacan Complex

The Oaxacan Complex is the largest Mesoproterozoic granulite exposure of Mexico (Figure 1c) and consists of locally migmatized ortho- and paragneisses. These sequences were intruded by abundant AMCG series and were subsequently metamorphosed under granulite facies conditions. For more details the reader is referred to Keppie *et al.* (2003, 2001) and Solari *et al.* (2004, 2003). For this study, zircons from three samples were analyzed.

Oax3-10-1 is from the type locality of the El Catrín (migmatite) unit of the northern Oaxacan Complex (Solari *et al.*, 2003) along the federal road from Oaxaca to Mexico (17°16'35"N, 96°58'15"W; Figure 1c). The El Catrín unit is of particular interest because previous ID-TIMS work (Solari *et al.*, 2003) yielded a ~1.4 Ga upper concordia intercept age and a lower intercept at ~1.1 Ga, which was interpreted as time of migmatization. The sample is from the dark grey paleosome and is a granulite with granoblastic equigranular texture. It contains mainly plagioclase, ortho- and clinopyroxene and brown hornblende. Quartz and K-feldspar are minor constituents together with opaque minerals and accessories apatite and zircon.

Oax3-10-2 is a quartzofeldspathic paragneiss from the El Marquez structural unit (17°13'54"N, 97°00'24"W) that is thrust over the El Catrín migmatite by a mylonitized contact zone (Solari *et al.*, 2003). The sample consists mainly of banded quartz and perthitic K-feldspar. Plagioclase is a minor constituent and no mafic minerals could be

observed in thin section, except for very small (~0.1 mm) euhedral garnet that occurs sporadically within the quartz bands. Accessory sillimanite is mostly retrogressed to white mica. Large apatite and zircon are accessories together with rare opaque minerals and secondary iron hydroxide.

*Oax113011* is a banded paragneiss from the Pluma Hidalgo area of the southern Oaxacan Complex (15°56'72"N; 96°14'92"W). The sample consists of quartz, clinopyroxene, K-feldspar and plagioclase. Most of the pyroxene is retrogressed to pale green hornblende. Other secondary phases are epidote, zoisite, calcite and chlorite. Euhedral titanite crystals are abundant and opaque minerals are another minor phase. The retrogression was accompanied by ductile deformation leading to dynamic recrystallization of quartz. The outcrop is in close vicinity to calcsilicate rocks suggesting that it is part of a supracrustal unit. However, a volcanosedimentary precursor cannot be excluded.

### The Guichicovi Complex

The Guichicovi Complex covers an area of ca. 400 km<sup>2</sup> west of the Tehuantepec Isthmus, Oaxaca (Figure 1c), and was first described by Murillo-Muñetón (1994). Geologic mapping (Weber and Hecht, 2003; Weber and Köhler, 1999) identified different metagneous series in the north and west that can be distinguished from supracrustal rocks exposed in the southeastern part of the complex. The Guichicovi Complex contains 1.25–1.20 Ga magmatic-arc protoliths similar to those found in rocks of the Oaxaquia microcontinent (Weber and Köhler, 1999; Weber and Hecht, 2003). Granulite facies metamorphism reached peak conditions at ~7.4 kb and ~840 °C (Murillo-Muñetón, 1994) at ~990–970 Ma (U-Pb zircon, Ruiz *et al.*, 1999; Weber and Köhler, 1999), followed by an amphibolite facies overprint at ~770°C (Cruz-Uribe *et al.*, 2014) locally with anatexis (Weber and Hecht, 2003). Cooling of the Guichicovi Complex is documented by Sm-Nd garnet-whole rock ages at ~933–911 Ma and Rb-Sr biotite-whole rock ages between ~882 and ~866 Ma (Weber and Köhler, 1999).

A Sm-Nd whole rock isochron of the metagneous suite whose slope corresponds to an age of 1.44 ± 0.08 Ga is indicative of a Mesoproterozoic depleted mantle source (Weber and Köhler, 1999). Depleted mantle Nd model ages (TDM<sub>(Nd)</sub>) of metasedimentary rocks vary from 2.0 to 1.5 Ga, indicating an older cratonic detrital component in some of the rocks. For this study the metasedimentary rocks with the oldest TDM<sub>(Nd)</sub> model ages (2.0–1.9 Ga, Weber and Köhler, 1999) were revisited and sampled for detrital zircon analyses.

Samples *Gui3-6-5* and *Gui3-6-6* (16°55'54"N, 95°05'34"W) are two varieties from the same outcrop southeast of Guichicovi. *Gui3-6-5* is composed of perthitic K-feldspar, quartz and light greenish clinopyroxene. Less abundant mineral phases are reddish-brown orthopyroxene and plagioclase. The rock is fine- to medium grained with a granoblastic equigranular texture having limited compositional banding. Euhedral titanite is an abundant accessory phase as well as anhedral primary (?) carbonate, apatite and zircon. Secondary phases are fine-grained carbonate, sericite and zoisite. Sample *Gui3-6-6* is a graphite-rich variety, which is composed mainly of granoblastic, perthitic K-feldspar with secondary flame-perthite structures and quartz. Orthopyroxene is more abundant than clinopyroxene. Minor components are graphite laths and plagioclase. Euhedral rutile and relatively large apatite crystals are accessories minerals together with zircon.

## ANALYTICAL METHODS

### LA-MC-ICPMS

The U-Pb geochronology of zircon grains by laser ablation multicollector inductively coupled plasma mass spectrometry (LA-MC-

ICPMS) was conducted at the Arizona LaserChron Center following the procedures given by Gehrels *et al.* (2008) and Johnston *et al.* (2009). Ablation was performed with a Photon Machines Analyte G2 Excimer laser (samples *Oax3-10-1*, *-2*, *Oax113011*, *Gui3-6-5*, *-6*) or a New Wave UP193HE Excimer laser (*Mol9-1*, *Mol9-4* to *Mol9-8*) using spot diameters of 30, 25 or 10 µm. The ablated material was carried with helium gas into the plasma source of a Nu HR ICPMS, which is equipped with a flight tube of sufficient width in order to analyze U, Th and Pb isotopes simultaneously. All measurements are made in static mode. For 30 and 25 µm spot analyses Faraday detectors with 3 × 10<sup>11</sup> ohm resistors were used for <sup>238</sup>U, <sup>232</sup>Th, <sup>208</sup>Pb–<sup>206</sup>Pb and discrete dynode ion counters for <sup>204</sup>Pb and <sup>202</sup>Hg. For a spot diameter of 10 µm Faraday detectors were used for <sup>238</sup>U, <sup>232</sup>Th and Channeltron detectors for <sup>208</sup>–<sup>204</sup>Pb.

<sup>204</sup>Hg interference with <sup>204</sup>Pb is accounted for measurement of <sup>202</sup>Hg during laser ablation and subtraction of <sup>204</sup>Hg according to the natural <sup>202</sup>Hg/<sup>204</sup>Hg ratio of 4.35. Common Pb correction is accomplished by using the measured <sup>204</sup>Pb and assuming an initial Pb composition from Stacey and Kramers (1975) with uncertainties of 1.0 for <sup>206</sup>Pb/<sup>204</sup>Pb and 0.3 for <sup>207</sup>Pb/<sup>204</sup>Pb. In-run analysis of fragments of a large zircon crystal (generally every fifth measurement) of known age (563.5 ± 3.2 Ma, 2σ, Gehrels *et al.*, 2008) is used to correct for fractionation. Uncertainty resulting from calibration corrections and the error on the external standard yields a total error of 1.0–1.5% (2 standard error) here referred to as systematic error (Gehrels *et al.*, 2008; Johnston *et al.*, 2009). This systematic error is added in quadrature to analytical errors to calculate the total age uncertainty.

### Lu-Hf isotope analysis by Isotope Dilution MC-ICPMS

Chemical preparation and element separation was performed in PicoTrace® cleanbenches (class 10 or better) at Laboratorio Ultralimpio de Geología Isotópica, Departamento de Geología (CICESE). Individual zircon grains, previously dated by LA-ICPMS, were chosen by either homogeneity or inheritance criteria, removed from mounts under a stereomicroscope with a needle and weighed on a Mettler microbalance at Oceanography Division (CICESE). Zircons were transferred into microcapsules, washed several times with warm 7 M HNO<sub>3</sub> and then with cold concentrated HNO<sub>3</sub>. Next, a <sup>180</sup>Hf-<sup>176</sup>Lu spike was pipetted into the microcapsules before adding about 0.5 ml of concentrated HF. Ten closed microcapsules were heated with HF as a pressure medium in a Parr bomb for 6 days at 180 °C. After digestion, the samples were dried down on a hotplate. Sample-spike equilibration was facilitated by adding 6 M HCl to the microcapsules, closing them, then heating overnight before drying down the sample again. Sample residues were then dissolved in ~0.5 ml of 1 M HCl and loaded to microcolumns filled with ~160 µl of Eichrom Ln-spec resin. Lu+Yb and Hf were eluted following a single column separation procedure adopted from (Nebel-Jacobsen *et al.*, 2005).

Hafnium and Lu isotope measurements were performed using the Micromass IsoProbe MC-ICPMS at Institut für Mineralogie, Münster University, Germany, following the procedure described in Weber *et al.* (2010). Measured Hf isotope ratios were corrected for instrumental mass bias using <sup>179</sup>Hf/<sup>177</sup>Hf = 0.7325 and the exponential law. All <sup>176</sup>Hf/<sup>177</sup>Hf values are reported relative to a value of 0.282160 for the Münster Hf standard, which is isotopically equivalent to the JMC-475 standard. To estimate the external reproducibility of samples, replicate analyses of the Hf standard at different concentrations (40, 80 and 120 ppb) were performed. The 2s.e. of cycles within single analyses correlates with the 2s.d. external reproducibility of multiple analyses, such that the external 2s.d. reproducibility is typically two to four times the 1s.e. internal run statistic (Bizzarro *et al.*, 2003). For Lu isotope dilution measurements, the Yb interference was corrected using the method outlined in Blichert-Toft *et al.* (2002) and the mass

Table 1. Lu-Hf data of zircons.

Sample ID	Weight (mg)	Lu (ppm)	Hf (ppm)	Lu-Hf isotope ratios					age corrected <sup>(b)</sup>			Model Age <sup>(d)</sup>	
				$^{176}\text{Lu}/^{177}\text{Hf}$	$\pm 2\text{s.d.}\%$ ext. rep. <sup>(a)</sup>	$^{176}\text{Hf}/^{177}\text{Hf}$	$\pm 2\text{s.e.} \times 10^6$ ( $2\sigma_m$ )	$\epsilon_{\text{Hf}}$	t (Ma)	$^{176}\text{Hf}/^{177}\text{Hf}(t)$	$\epsilon_{\text{Hf}}(t)$	$\pm 2\text{s.d.}\%$ ext. rep. <sup>(c)</sup>	TDM <sub>(Hf)</sub> (Ma)
<i>Mol9-1</i>													
2E	22.3	28	8860	0.000448	0.77	0.282175	6	-21.6	1211	0.282165	5.2	0.62	1628
2E(rep)	22.3	28	8860	0.000448	0.77	0.282165	7	-21.9	1211	0.282155	4.9	0.58	1650
<i>Mol9-4</i>													
13	19.8	27	9610	0.000396	0.68	0.282137	6	-22.9	1411*	0.282126	8.4	0.62	1581
13(rep)	19.8	27	9610	0.000396	0.68	0.282133	5	-23.0	1411*	0.282123	8.3	0.49	1588
1W	15.1	15	10400	0.000212	0.79	0.282129	5	-23.2	1411*	0.282124	8.4	0.56	1586
1J	10.5	12	8380	0.000196	0.91	0.282125	8	-23.3	1411*	0.282120	8.2	0.87	1595
12	9.4	31	10300	0.000422	0.69	0.282130	7	-23.2	1411*	0.282119	8.2	0.81	1597
<i>Mol9-5</i>													
2M	5.0	29	8450	0.000491	0.84	0.282076	11	-25.1	1412*	0.282063	6.2	0.70	1724
2S	3.2	47	10200	0.000650	0.73	0.282086	15	-24.7	1412*	0.282068	6.4	0.85	1712
3B	5.0	28	10700	0.000376	0.85	0.282086	11	-24.7	1412*	0.282076	6.7	0.73	1694
<i>Mol9-6</i>													
2F	20.8	31	8770	0.000507	0.72	0.282194	6	-20.9	1200	0.282182	5.6	0.68	1595
2R	9.5	31	8800	0.000497	0.74	0.282176	7	-21.5	1212	0.282165	5.3	0.74	1627
2A	6.9	35	9570	0.000514	0.78	0.282191	9	-21.0	1207	0.282179	5.7	0.99	1598
<i>Oax3-10-1</i>													
3F	19.6	35	10600	0.000468	0.71	0.282161	6	-22.1	1208	0.282150	4.7	0.62	1662
3W	4.2	151	11300	0.001898	0.62	0.282111	11	-23.8	1405	0.282061	6.0	0.73	1734
3V	5.6	32	12700	0.000356	0.87	0.282106	8	-24.0	1256	0.282098	3.9	0.60	1750
<i>Oax3-10-2</i>													
3K	4.3	197	15300	0.001829	0.62	0.282134	10	-23.0	1074	0.282097	-0.3	0.66	1871
3J	29.3	111	7400	0.002127	0.62	0.282172	6	-21.7	1206	0.282124	3.7	0.68	1724
3I	12.5	201	13000	0.002201	0.63	0.282175	6	-21.6	1209	0.282125	3.8	0.62	1720
32	10.0	184	14300	0.001820	0.63	0.282148	4	-22.5	1222	0.282106	3.4	0.43	1753

(a) Estimated %2s.d. external reproducibility of the  $^{176}\text{Lu}/^{177}\text{Hf}$  value including error magnification from sub-optimal tracer-sample ratios; for external reproducibility on  $^{176}\text{Hf}/^{177}\text{Hf}$  see text. (b)  $^{176}\text{Hf}/^{177}\text{Hf}(t)$  and  $\epsilon_{\text{Hf}}(t)$  are calculated using  $^{207}\text{Pb}^*/^{206}\text{Pb}^*$  age of zircon cores except zircons from samples Mol9-4 and Mol9-5 upper intercept ages of igneous protoliths were used (\*). Epsilon Hf is the deviation of  $^{176}\text{Hf}/^{177}\text{Hf}$  of the sample relative to the chondritic uniform reservoir (CHUR) times  $10^4$ . For the calculations present-day CHUR values  $^{176}\text{Hf}/^{177}\text{Hf}_{\text{CHUR}(0)} = 0.282785$  and  $^{176}\text{Lu}/^{177}\text{Hf}_{\text{CHUR}} = 0.0336$  (Bouvier *et al.*, 2008) were used. (c) Total propagated uncertainty, including the estimated 2s.d. external reproducibilities (see text) of both the  $^{176}\text{Hf}/^{177}\text{Hf}$  and  $^{176}\text{Lu}/^{177}\text{Hf}$  values. The age uncertainty is not included in the error propagation. (d) Two-stage crustal residence model ages were calculated thus:  $t_{\text{DM}} = (1/\lambda)\ln(1+m)$ , where  $m = \{(^{176}\text{Hf}/^{177}\text{Hf})_{\text{DM}} - [(^{176}\text{Hf}/^{177}\text{Hf})_{\text{zirc}} + (^{176}\text{Lu}/^{177}\text{Hf})_{\text{avg. crust}}(e^{\lambda t} - 1)]\} / \{(^{176}\text{Lu}/^{177}\text{Hf})_{\text{DM}} - (^{176}\text{Lu}/^{177}\text{Hf})_{\text{avg. crust}}\}$ . We assumed  $(^{176}\text{Lu}/^{177}\text{Hf})_{\text{avg. crust}} = 0.015$  (Condie *et al.*, 2005). The present day depleted mantle model is based on  $(^{176}\text{Hf}/^{177}\text{Hf})_{\text{DM}} = 0.283224$  (Vervoort *et al.*, 2000) and  $(^{176}\text{Lu}/^{177}\text{Hf})_{\text{DM}} = 0.03836$  Weber *et al.*, 2010). rep: replicate analysis.

bias was corrected using admixed Re (Scherer *et al.*, 2001). In Table 1, the uncertainties have been expanded to include the effects of over- or underspiking for Lu. Crustal residence ages were calculated in two-steps: (1) using  $^{176}\text{Lu}/^{177}\text{Hf}$  of the zircon to calculate the Hf isotope evolution from present day to the crystallization age; and (2) for the time before the zircon crystallization age Hf isotope evolution was calculated by assuming  $^{176}\text{Lu}/^{177}\text{Hf}$  of 0.015 for average crust. For the present day depleted mantle model  $^{176}\text{Hf}/^{177}\text{Hf} = 0.283224$  (Vervoort *et al.*, 2000) and  $^{176}\text{Lu}/^{177}\text{Hf} = 0.03836$ , calculated for  $\epsilon_{\text{Hf}} = 0$  at 4500 Ma by using  $\lambda = 1.867 \times 10^{-11}\text{a}^{-1}$  (Scherer *et al.*, 2001; Söderlund *et al.*, 2004).

## RESULTS

### Metaigneous rocks from the Huiznopala Gneiss

The gabbro sample *Mol9-1* contains relatively large (>200 $\mu\text{m}$ ), mostly round or elliptic zircons with anhedral, patchy internal structures (Figure 3e-3h) and minor development of magmatic zoning (Figure 3d). Forty-one 30  $\mu\text{m}$  laser spots yield apparent  $^{207}\text{Pb}/^{206}\text{Pb}$  ages ranging from ~1269 to ~993 Ma (see Appendix 1 of the electronic

supplement). Upper and lower concordia intercept ages were calculated at  $1189 \pm 52$  and  $950 \pm 88$  Ma, respectively (Figure 3a). The upper intercept age corresponds to the time of igneous zircon crystallization and the lower intercept reflects ancient Pb loss or metamorphic zircon growth. Most of the data plot around either 1200 or 1045 Ma as indicated by the probability peaks shown in Figure 3b. The older zircon zones are clearly inherited from an igneous protolith as indicated for instance by a zircon with igneous zoning and minor overgrowth shown in Figure 3d of which three spots yielded *ca.* 1.2 Ga, or by corroded cores of similar age with younger overgrowth (Figures 3e, 3f, 3h). A probability peak at 1045 Ma (Figure 3b) is presumably of no geologic significance. It is noteworthy, however, that 11 laser spots either on zircon overgrowth (Figure 3f), cores (Figure 3j) or unzoned zircon yield ages in a narrow range from 1050 to 1038 Ma. On the other hand, data from the youngest four spots yield a concordia age of  $1015 \pm 13$  Ma (Figure 3c), which might be a better estimate for an age with geologic significance, probably high-grade metamorphism. It remains unclear, however, if all intermediate concordant ages are mixed ages due to a partially reset of the isotopic system or they correspond to the anorthosite forming igneous event shortly prior to granulite fa-

cies metamorphism as supposed from other Grenvillian exposures in Mexico (e.g. Cameron *et al.*, 2004; Weber *et al.*, 2010; Schulze, 2011). If the latter is true, then the gabbroic patches in the anorthosite are either xenoliths from an older (1.2 Ga) lower crust or they are gabbroic “Schlieren”, being the result of differentiation of the anorthositic magma that was produced by melting of ~1.2 Ga lower crust. One zircon grain (2E, Table 1, Figure 3f) was analyzed for Lu-Hf isotopes by solution MC-ICPMS. The  $^{177}\text{Hf}/^{176}\text{Hf}$  value, recalculated to the age of the zircon core at 1211 Ma, is 0.28216, which corresponds to an  $\epsilon\text{Hf}_{(1211\text{Ma})}$  of  $+5.1 \pm 0.6$  and a two step  $\text{TDM}_{(\text{Hf})}$  model age of 1.64 Ga.

The magmatic orthogneiss sample *Mol9-4* from the Main Series contains big (>200  $\mu\text{m}$ ) mostly elliptic zircon with oscillary zoning in its interior. This zoned zircon is in many cases corroded or broken and overgrown by either, low luminescent (U-rich) or highly luminescent (U-poor granulite facies) zircon or both. The metamorphic overgrowths are extremely small (mostly <10  $\mu\text{m}$ ) or totally absent (see CL images Figures 4e-4h with no visible metamorphic overgrowth). Laser ablation MC-ICPMS analyses with 10  $\mu\text{m}$  beam size were focused on the magmatic zircons. Twenty-eight out of 38 laser spot analyses yielded apparent  $^{207}\text{Pb}/^{206}\text{Pb}$  minimum ages, above 1.3 Ga with a probability peak at 1350 Ma (Figure 4b). An upper concordia intercept age of  $1411 \pm 27$  Ma was calculated from 24 laser spot data (Figure 4a, red ellipses with solid lines). This age is interpreted as the best estimate for the time of crystallization for the magmatic protolith. Four slightly older, discordant ages that indicate some inheritance as well as eight

younger data (Figure 4a, blue and yellow ellipses with stippled lines) were excluded from this calculation. Several laser spots performed on these grains suggest that most of the zircons reflects the protolith age and no significant age differences occurs from inner core to outer zones (not rims). For instance, Figures 4c and 4d show the results from two individual zircon grains with four laser spots analyzed across each of them (Figures 4e and 4f). The data yield a concordant age at  $1333 \pm 36$  and a concordia intercept age at  $1401 \pm 120$  Ma, respectively. Laser spots that yield younger ages reflect the effects of migmatization and metamorphism between ~1.2 and ~1.0 Ga but no further interpretation is possible. Figures 4e to 4h show CL images of those zircon grains that were analyzed for Lu-Hf isotopes. Hafnium isotope compositions of these zircon grains (13, 12, 1W, 1J, Table 1) yield within errors identical initial  $^{177}\text{Hf}/^{176}\text{Hf}$  values of 0.282119–0.282126 corresponding to  $\epsilon\text{Hf}_{(1411\text{Ma})}$  from +8.2 to +8.4 and  $\text{TDM}_{(\text{Hf})}$  model ages from 1.60 to 1.58 Ga.

Zircon grains from the garnet-bearing orthogneiss *Mol9-5* are short to long prismatic with aspect ratios from 1:2 to 1:6. The complexity of these zircons can be observed from CL images (Figures 5e-5i). Some zircon grains display several generations of zircon like inherited cores surrounded by zircon with magmatic zoning and metamorphic rims. Partly corroded magmatic zones with metamorphic overgrowth give zircon grains an oval or elliptic aspect. Most zircons are less than 200  $\mu\text{m}$  in size with 10–20  $\mu\text{m}$  metamorphic rims. Thirty-eight 10  $\mu\text{m}$  laser spot analyses yield  $^{207}\text{Pb}/^{206}\text{Pb}$  ages from ~1945 to ~1063 Ma

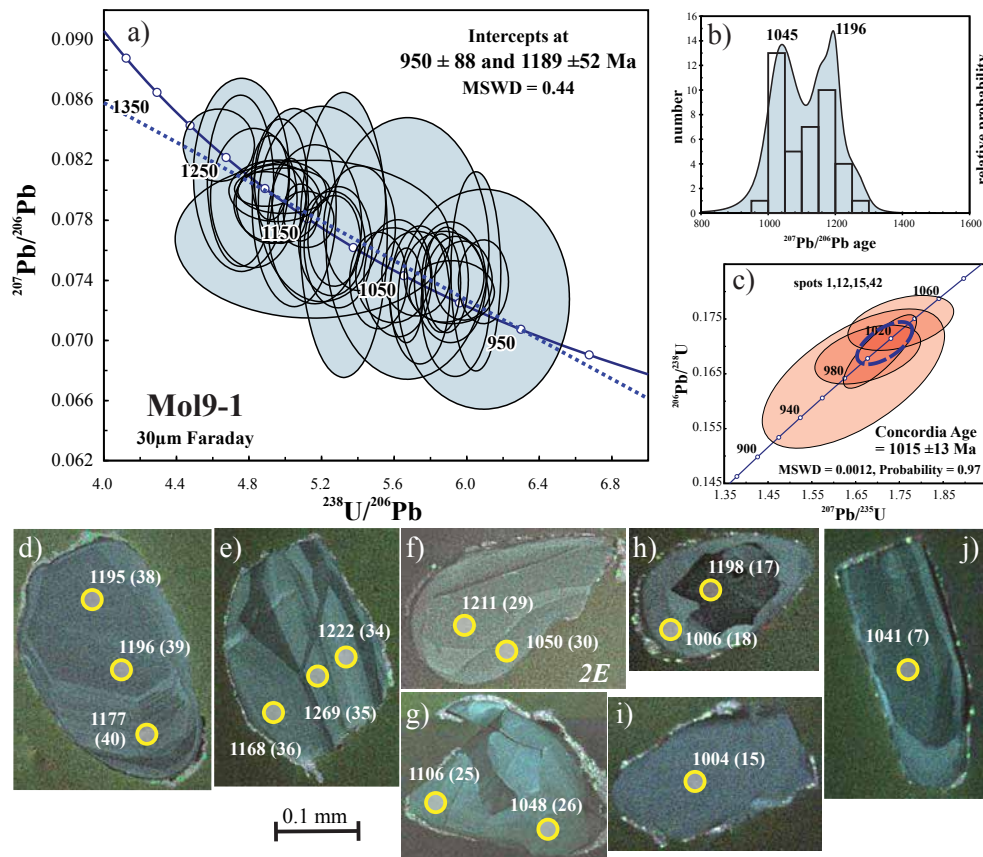


Figure 3. Zircon data of gabbro sample *Mol9-1*. (a) Tera-Wasserburg diagram of U-Pb isotope ratios analyzed by LA-MC-ICPMS. (b) Histogram and relative probability plot of apparent  $^{207}\text{Pb}/^{206}\text{Pb}$  ages; (c) concordia diagram showing concordant laser spot analyses (spot numbers from data table of *Mol9-1* in Appendix 1) that may correspond to anorthosite magmatism. (d-j) Cathodoluminescence (CL) images of typical zircons showing positions, apparent  $^{207}\text{Pb}/^{206}\text{Pb}$  ages and, (in parenthesis) analysis number from data table of *Mol9-1* in Appendix 1 of the electronic supplement. (f) *Italic 2E* is sample identifier of zircon removed from mount and analyzed by dilution MC-ICPMS for Lu-Hf isotopes (see Table 1). Note: All errors, error ellipses, and bars are  $2\sigma$ .

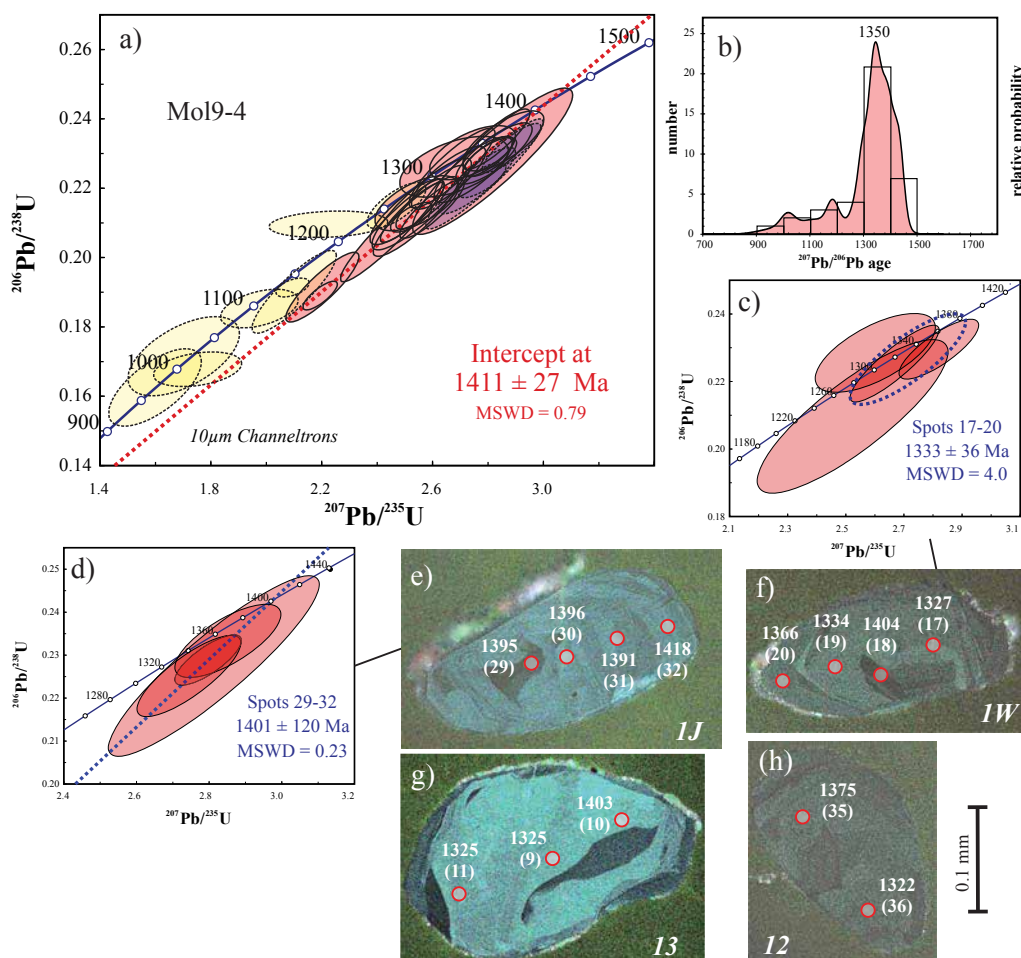


Figure 4. Zircon data of migmatic orthogneiss sample *Mol9-4* from the Main Series. (a) Concordia diagram of all laser data. Intercept age calculated from a group of 24 laser analyses (red error ellipses with solid lines), blue ellipses were omitted from age calculation due to older inheritance. (b) Histogram and relative probability plot of apparent  $^{207}\text{Pb}/^{206}\text{Pb}$  ages. (c, d) Concordia diagrams of laser spot data from individual zircons shown in (c) and (d), respectively. (c – concordia age, d – upper intercept age). (e–h) CL images of typical zircon grains showing positions of spot analyses, apparent  $^{207}\text{Pb}/^{206}\text{Pb}$  ages, and (in parenthesis) analysis number from data table of *Mol9-4* in Appendix 1 of the electronic supplement. *Italic* numbers are sample identifier of zircon grains removed from mount and analyzed by dilution MC-ICPMS for Lu-Hf isotopes (see Table 1). Note: All errors, error ellipses, and bars are  $2\sigma$ .

with a major probability peak at 1390 Ma (Figure 5b). In the concordia diagram of Figure 5a red error ellipses represent the magmatic zones, whereas green and blue ellipses correspond to inherited cores. Two magmatic phases are clearly distinguished (Figures 5c, 5d), the younger yielding a concordia age at  $1243 \pm 7$  Ma and the older with an intercept age at  $1412 \pm 59$  Ma. The CL images show (1) the presence of inherited cores within the  $\sim 1.4$  Ga magmatic zircon (Figures 5e, 5h) and (2)  $\sim 1.24$  Ga magmatic zircon growth around the  $\sim 1.4$  Ga cores (Figure 5g). This implies crustal anatexis at *ca.* 1.24 Ga leading to granitoids with S-type characteristics, an interpretation which is also supported by the presence of garnet in this rock.

Two inherited core ages can be distinguished: (1) two analyses from different grains are almost concordant at *ca.* 1.7 Ga and another zircon core is discordant with a similar  $^{207}\text{Pb}/^{206}\text{Pb}$  age (blue error ellipses and dot in Figures 5a, 5h); (2) four laser spot analyses performed on another complex zircon yielded discordant ages with upper and lower concordia intercepts at  $2026 \pm 59$  Ma and  $1089 \pm 58$  Ma, respectively, the former indicating a Paleoproterozoic age of the core.

Lutetium-hafnium analyses were performed from three grains (2M, 2S, and 3B shown in Figure 5f, 5h, and 5i). The Hf isotope data were recalculated to the age of the magmatic protolith, best estimated at

1412 Ma. The zircons yield within errors identical initial  $^{177}\text{Hf}/^{176}\text{Hf}_{(1412)}$  from 0.282063 to 0.282076, that correspond to  $\epsilon\text{Hf}_{(1412)}$  from +6.2 to +6.7 and  $\text{TDM}_{(\text{Hf})}$  from 1.72 to 1.69 Ga (Table 1) which are significantly older than those from samples *Mol9-1* and *Mol9-4*. Surprisingly, the Hf isotopic composition of grain 2S, having a 1.7 Ga inherited core, is indistinguishable from the other two grains without such old core, suggesting that Hf comes mainly from older, pre-existing zircon with no significant radiogenic growth of  $^{176}\text{Hf}$  by  $^{176}\text{Lu}$  decay. This means that no external radiogenic Hf from the whole rock, which has by average a twentyfold Lu-Hf ratio compared to zircon, was added to the zircon during magmatic growth.

#### Huiznopala Supracrustal Unit

A total of 232 zircon grains from samples of the Huiznopala Supracrustal Unit were analyzed by LA-MC-ICPMS. Many of these zircon grains are relatively large ( $>500 \mu\text{m}$ ) and display well developed oscillatory zoning with only minor metamorphic overgrowth (Figure 6a.). None of the analyzed zircon grains have a  $^{207}\text{Pb}/^{206}\text{Pb}$  age older than 1.3 Ga (Figure 6). Zircons from sample *Mol9-6* have a single probability peak at 1210 Ma similar to sample *Mol9-8* with a major peak at 1235 Ma. Zircon grains from sample *Mol9-7* tend to have younger ages with

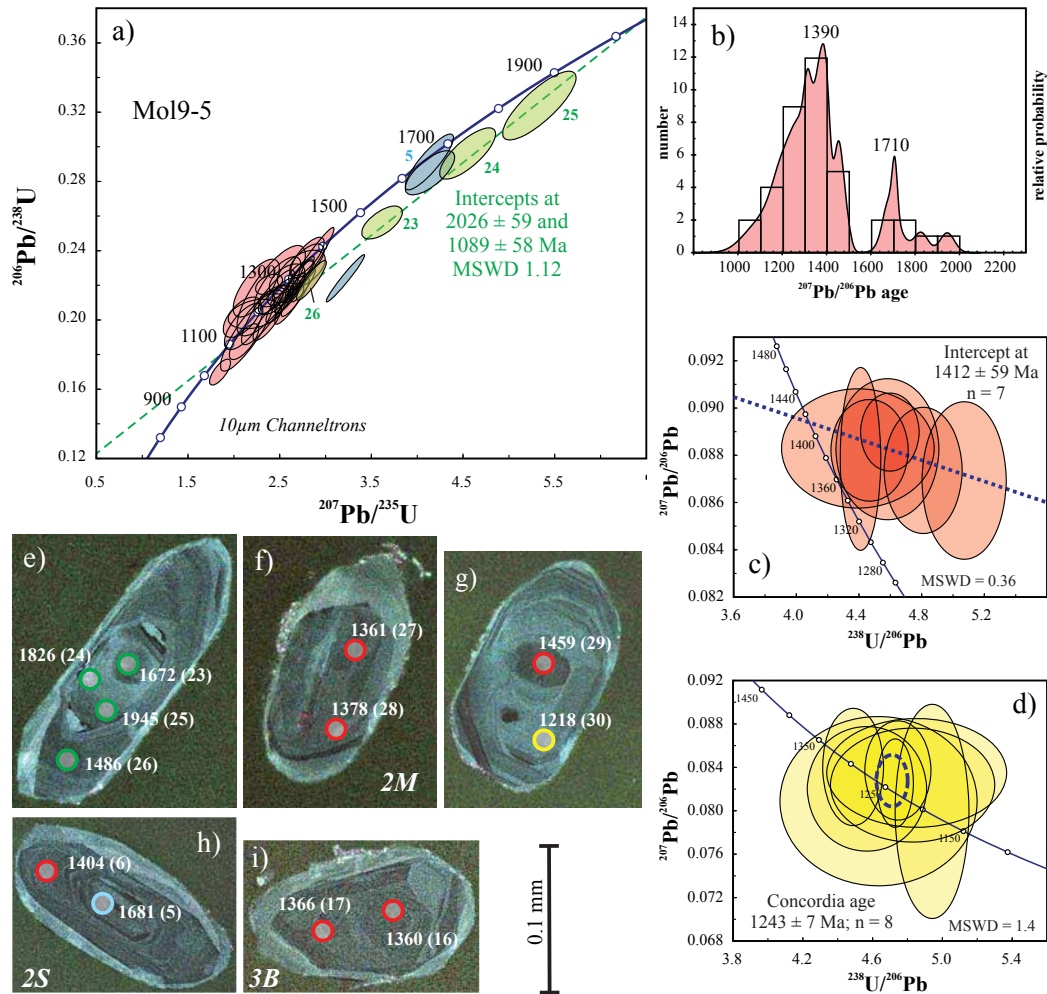


Figure 5. Zircon data of garnet-bearing orthogneiss sample *Mol9-5* from the Main Series. (a) Concordia diagram of all laser data. Dashed (green) discordia line and intercept ages calculated from four laser spot analyses (green ellipses) of the zircon grain shown in (e). Blue ellipses are from ca. 1.7 Ga inherited cores (like in h). (b) Histogram and relative probability plot of apparent  $^{207}\text{Pb}/^{206}\text{Pb}$  ages. (c, d) Tera-Wasserburg diagrams of ca. 1.4 (c) and ca. 1.24 (d) groups of igneous zircon growth zones. (e-i) CL images of typical zircon grains showing positions of spot analyses, apparent  $^{207}\text{Pb}/^{206}\text{Pb}$  ages, and (in parenthesis) analysis number from data table of *Mol9-5* in Appendix 1 of the electronic supplement. *Italic* numbers as in Figure 4. Note: All errors, error ellipses, and bars are  $2\sigma$ .

less pronounced probability peaks at 1165 and 1103 Ma. One third of the analyzed laser spots on sample *Mol9-7* yield  $^{207}\text{Pb}/^{206}\text{Pb}$  ages below 1.0 Ga yielding a probability peak at 983 Ma (blue error ellipses and probability peaks in Figure 6d and 6e). The maximum depositional age of the sediments is difficult to establish as ancient Pb-loss during the time of granulite facies metamorphism affected many of the analyzed zircon grains.

Three zircon grains from sample *Mol9-6* (2R, 2F, 2A, Figure 6a) were analyzed for Lu-Hf isotopes. The Hf-isotope ratios were recalculated to the  $^{207}\text{Pb}/^{206}\text{Pb}$  minimum crystallization ages of the corresponding laser spots. The initial  $^{177}\text{Hf}/^{176}\text{Hf}$  values range from 0.282165 to 0.282182 (Table 1). The corresponding  $\epsilon_{\text{Hf}(t)}$  values range from +5.3 to +5.7 and the TDM<sub>(Hf)</sub> model ages from 1.63 to 1.60 Ga indicating these grains crystallized from a similar crustal source.

### The Oaxacan Complex migmatite and paragneisses

Compared to the other samples of this study, zircon is less abundant in the El Catrín migmatite paleosome sample *Oax3-10-1* and mostly <200  $\mu\text{m}$  in size. The CL images reveal several growth zones (Figure 7f) with no or less pronounced oscillatory zoning. Forty-seven 30  $\mu\text{m}$

laser spot analyses were conducted on zircon cores and overgrowth, avoiding metamorphic rims. Red error ellipses in the Wetherill concordia plot of Figure 7a are from zircon cores with apparent  $^{207}\text{Pb}/^{206}\text{Pb}$  ages older than 1.3 Ga, corresponding to the crystallization age of the protolith. An upper concordia intercept calculated from 14 laser spots (forced to an age of metamorphism at 990 Ma to its lower end; Solari *et al.*, 2003) yields an age of  $1444 \pm 54$  Ma. This protolith age can be further improved by using the four oldest concordant spots that yield a concordia age of  $1444 \pm 16$  Ma (Figure 7b), which is considered the best estimate for protolith crystallization. The isotope data from laser spots on younger zircon zones surrounding the cores on CL images (yellow error ellipses in Figure 7a) can be separated into two sets (Figures 7c, 7d, 7e): (1) twelve analyses that correspond to an upper intercept age of  $1271 \pm 67$  Ma (Figure 7c) and (2) another 12 analyses that yield a concordia age at  $1116 \pm 14$  Ma (Figure 7d). As the error ellipses of all analyzed laser spots plot along the concordia it is speculative to separate these age groups, especially the latter at  $1116 \pm 14$  Ma. The presence of  $\sim 1.44$  Ga cores is evident, as well as  $\sim 1.27$  Ga igneous crystallization that is documented by the upper intercept age of all data except those from the inherited cores (Figure 7a, blue discordia). Granulite facies

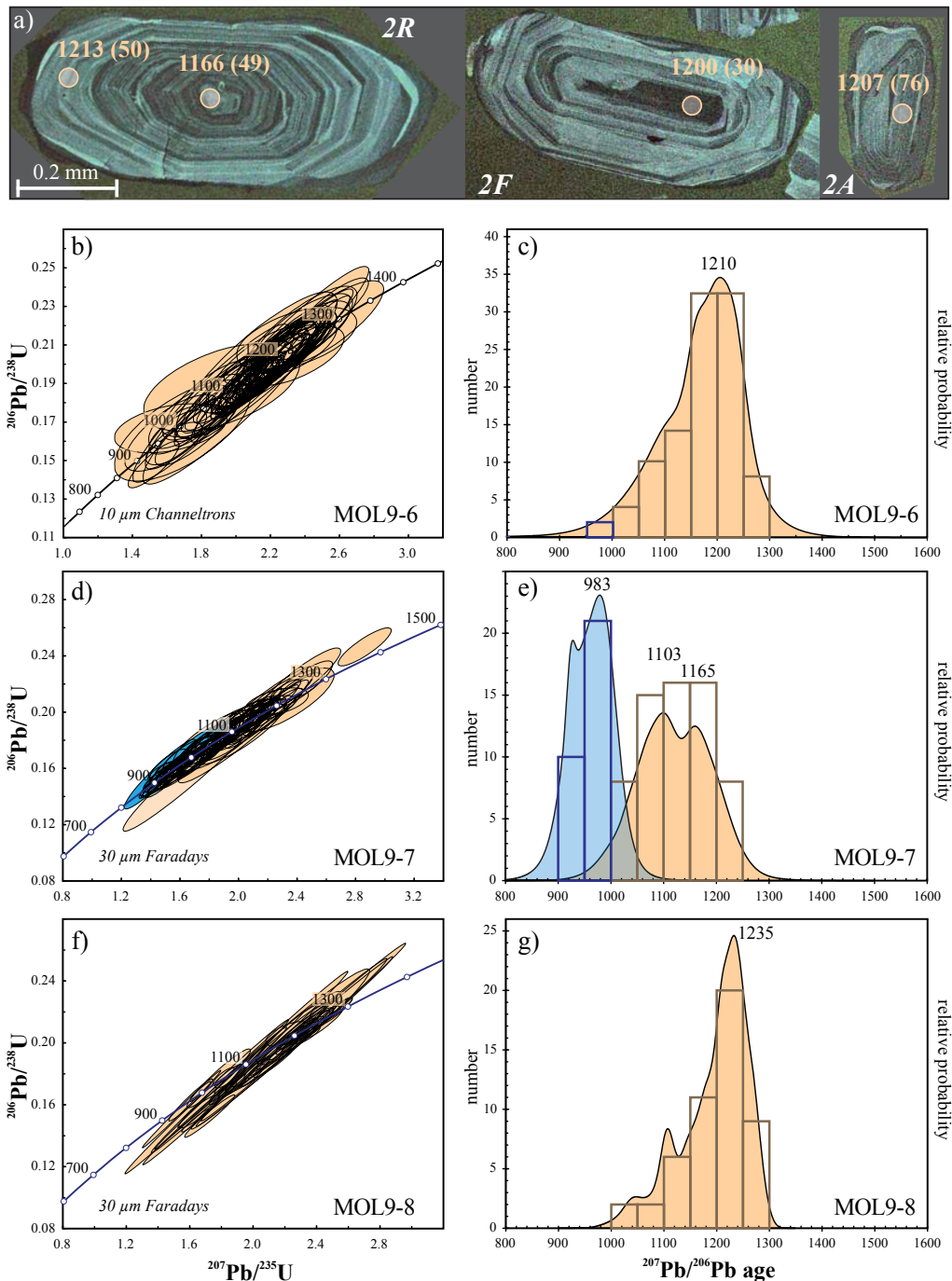


Figure 6. Zircon data of paragneiss samples from the Huiznopala Supracrustal Unit. (a) CL images of typical zircon grains showing positions of spot analyses, apparent  $^{207}\text{Pb}/^{206}\text{Pb}$  ages, and (in parenthesis) analysis number from data table of *Mol9-6* in Appendix 1 of the electronic supplement. *Italic* numbers as in Figure 4. (b, d, f) concordia diagram and (c, e, g) histogram and relative probability plot of apparent  $^{207}\text{Pb}/^{206}\text{Pb}$  ages. Note: Blue error ellipses, histogram bars and probability plots correspond to the age of metamorphism and the data are not included for provenance analyses.

metamorphism at *ca.* 990 Ma is documented by Solari *et al.* (2003). Nonetheless, an additional tectonothermal event corresponding to the migmatite formation prior to granulite facies metamorphism is evident from zircon growth zones and from field observations. It cannot be resolved from the data presented here, whether the  $1116 \pm 14$  Ma concordia age corresponds to zircon growth during migmatization or if this is a mixed age. However, the result is in good agreement with

the age of the Olmecan event reported by Solari *et al.* (2003) from the El Catrín Unit.

Three zircons from sample *Oax3-10-1* were removed from the mount and analyzed for Lu-Hf isotopes (3F, 3V, and 3W, Figure 7f). The measured  $^{177}\text{Hf}/^{176}\text{Hf}$  values were recalculated to the  $^{207}\text{Pb}/^{206}\text{Pb}$  age of the oldest analyzed laser spot on the corresponding zircon grain (Figure 7f). The zircon grain with the ~1.4 Ga core (3W) has a  $^{177}\text{Hf}/^{176}\text{Hf}_{(1405)}$

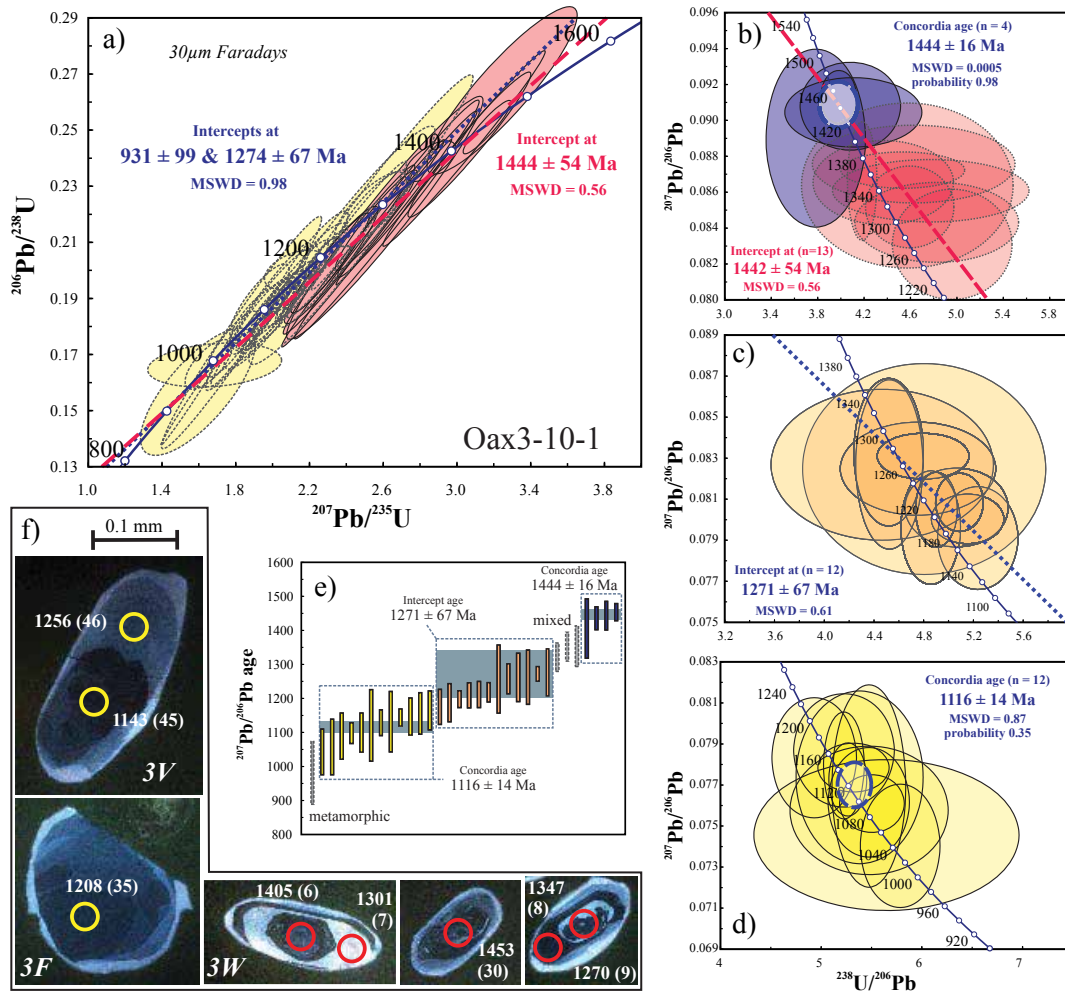


Figure 7. Zircon data of migmatite sample *Oax3-10-1* from the El Catrín migmatite of the northern Oaxacan Complex. (a) Concordia diagram of all analyzed laser spots. Dashed red discordia line is calculated from red error ellipses with solid lines (forced to  $990 \pm 10$  Ma lower intercept), blue stippled discordia line is calculated from yellow error ellipses with dashed lines. (b-d) Tera-Wasserburg diagrams of different age groups calculated as concordia or upper intercept ages (Ludwig, 2008); (e) same age groups as (b-d) illustrated by using apparent  $^{207}\text{Pb}/^{206}\text{Pb}$  ages. (f) CL images of typical zircon grains showing positions of spot analyses, apparent  $^{207}\text{Pb}/^{206}\text{Pb}$  ages, and (in parenthesis) analysis number from data table of *Oax3-10-1* in Appendix 1 of the electronic supplement. *Italic* numbers as in Figure 4. Note: All errors, error ellipses, and bars are  $2\sigma$ .

value of 0.282061, the  $\sim 1.2$  Ga grain (3F) without visible inheritance has a  $^{177}\text{Hf}/^{176}\text{Hf}_{(1208)}$  value of 0.282150, and the zircon grain 3V yielded  $^{177}\text{Hf}/^{176}\text{Hf}_{(1256)}$  of 0.282098 in-between the other two values (Table 1). The Hf isotope composition of the latter grain is considered to reflect a mixture of magmatic zircon and an inherited core observed on CL image. Two step  $\text{TDM}_{(\text{Hf})}$  model ages for these zircons are 1.75–1.73 Ga for the grains with cores and 1.66 Ga for grain 3F without core. The results suggest two different crustal sources being mixed during magmatic protolith formation.

Paragneiss sample *Oax3-10-2* from the El Marquez unit contains large ( $>500\mu\text{m}$ ), dark reddish-brown zircon. Many grains are rounded fragments of igneous zircon with metamorphic overgrowth (see CL images in Figure 8b). None of the 77 analyzed zircon grains yielded  $^{207}\text{Pb}/^{206}\text{Pb}$  ages older than 1222 Ma (Figures 8a, 8b). Major probability peaks of detrital zircons are at 1210 and 1179 Ma both in the range of typical Oaxaquia arc magmatism.

Four concordant zircon grains of sample *Oax3-10-2* were analyzed for Lu-Hf isotopes and the results were recalculated to the corresponding  $^{207}\text{Pb}/^{206}\text{Pb}$  age (3I, 3J, 3K, 32, Figure 8b). The  $^{177}\text{Hf}/^{176}\text{Hf}_{(i)}$  values range from 0.282097 to 0.282125. The  $\epsilon\text{Hf}_{(i)}$  values of zircon depend

significantly on the age to which the  $^{177}\text{Hf}/^{176}\text{Hf}_{(i)}$  value is recalculated. Thus, three *ca.* 1.2 Ga zircon have  $\epsilon\text{Hf}_{(1222-1206\text{Ma})}$  values from +3.4 to +3.8 and the younger grain with an  $^{207}\text{Pb}/^{206}\text{Pb}$  age of  $\sim 1074$  Ma yield  $\epsilon\text{Hf}_{(1074\text{Ma})}$  of -0.3. This difference is also reflected in the  $\text{TDM}_{(\text{Hf})}$  model ages ranging from 1.75 to 1.73 Ga for the first group of zircon and 1.87 Ga for the latter grain.

The paragneiss sample *Oax113011* from the southern Oaxacan Complex contains zircons with cores and several growth zones (Figure 8d). In most cases inherited cores are surrounded by oscillatory-zoned zircon and/or low luminescent (high U) zircon. Besides that high luminescent (low U) metamorphic rims are observed. The CL images are very similar to those of zircons from nearly exposed granulite facies migmatites (Weber *et al.*, 2010). Forty-one analyzed zircon cores yield a probability peak at 1176 Ma (Figure 7d). Six zircon core analyses yielded ages younger than 1000 Ma of which a concordia age value of  $959 \pm 11$  Ma was calculated (Figure 8a). The results indicate that some zircon cores were affected by complete Pb-loss during metamorphism. Thus, it is probable that most of the other cores suffered at least partial Pb-loss.

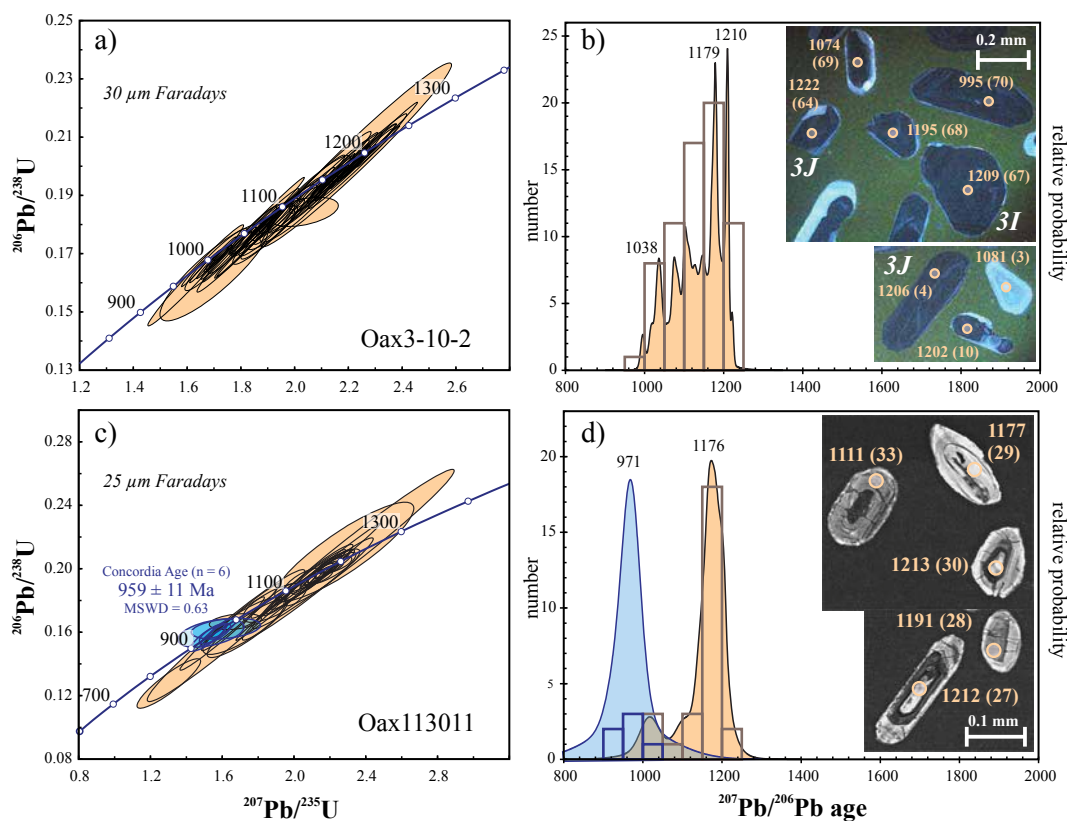


Figure 8. Zircon data of paragneiss samples from the Oaxacan Complex. (a, c) Concordia diagram and (b, d) histogram and relative probability plot of apparent  $^{207}\text{Pb}/^{206}\text{Pb}$  ages. Note: Blue error ellipses, histogram bars and probability plots correspond to the age of metamorphism and the data are not included for provenance analyses. CL images of typical zircon grains showing positions of spot analyses, apparent  $^{207}\text{Pb}/^{206}\text{Pb}$  ages, and (in parenthesis) analysis number from data table in Appendix 1 of the electronic supplement. *Italic* numbers as in Figure 4.

### Guichicovi Complex paragneiss

Zircons from samples *Gui3-6-5* and *Gui3-6-6* are mostly small ( $\sim 100\mu\text{m}$ ), rounded and elongated, often with complex internal structures and/or inherited fragments. The results are shown on a concordia diagram (Figure 9a) and a relative probability plot (Figure 9b) in which a group of six analyses were excluded. The latter yield a concordia age of  $978.0 \pm 5.3$  Ma reflecting the time of metamorphism (Figure 9a). Most of the  $^{207}\text{Pb}/^{206}\text{Pb}$  ages ( $n = 59$ ) are in the range from 1250 to 1000 Ma with a major peak at 1178 Ma. The remaining 29 analyses, mainly performed on zircon cores, are older with probability peaks at 1.33, 1.41–1.47, and 1.65 Ga. Many of these zircon cores yield discordant ages (yellow ellipses with stippled lines in Figure 9a), indicating that the corresponding  $^{207}\text{Pb}/^{206}\text{Pb}$  age is a minimum age for zircon crystallization. The 1.65 Ga peak, instead, is constrained by two concordant ages (see Figure 9c, spots 77 and 90). The oldest core (spot 19) yielded a strongly discordant  $^{207}\text{Pb}/^{206}\text{Pb}$  age of  $\sim 1.9$  Ga. Forced to the age of metamorphism at *ca.* 978 Ma an upper intercept will reach  $2.6 \pm 0.5$  Ga, suggesting influence from an early Paleoproterozoic or Archean craton.

## DISCUSSION

### Significance of early Mesoproterozoic magmatism

The new data presented here, together with previously reported ID-TIMS upper intercept ages (Schulze, 2011), show that 1.4–1.5 Ga ages are not uncommon in Oaxaquia. In Table 2 all reported early Mesoproterozoic ages of metaigneous rocks from Oaxaquia are listed. Whereas Weber and Köhler (1999) interpreted a  $1.44 \pm 0.08$  Ga Sm-Nd

isochron of 16 metaigneous whole rocks from the Guichicovi Complex in terms of a major crust formation event, Lawlor *et al.* (1999) did not pay any further attention to a similar Sm-Nd isochron obtained from 12 whole rock samples of Huiznopala's Main Series. Solari *et al.* (2003) instead, interpreted upper concordia intercepts at  $\sim 1.4$  Ga from the El Catrín migmatite as a minimum age of protolith crystallization.

Samarium-neodymium whole rock isochrons typically have large errors due to insufficient isotopic homogenization in the precursor and small variations on Sm-Nd ratios between samples; hence, whole rock isochrons are of limited use to constrain the age of an igneous event. On the other hand, crust formation is indicated when the initial Nd isotope ratio corresponds to depleted mantle values from which crust forming magma is originally separated. The same concept is also used for depleted mantle model ages (TDM), which are commonly applied to compare crustal provinces (*e.g.*, Arndt and Goldstein, 1987; DePaolo, 1981). Most of the reported  $\text{TDM}_{(\text{Nd})}$  model ages of metaigneous rocks from Oaxaquia are between 1.6 and 1.4 Ga (Lawlor *et al.*, 1999; Ruiz *et al.*, 1988; Schulze, 2011; Weber and Köhler, 1999). The initial  $\epsilon\text{Nd}$  values of whole rock isochrons, instead, are around +4 to +5, which is below the depleted mantle model values at this time (Weber and Köhler, 1999). Given that Sm-Nd isochron ages reflect the time of magmatic separation from a mantle reservoir, this reservoir was less depleted than a depleted mantle model used for  $\text{TDM}_{(\text{Nd})}$  (like the DePaolo, 1981 model). It is widely accepted that Nd isotopic composition of oceanic island arcs are below those of typical DM, due to mixing of subducted ocean floor sediments into the generation of arc magmas (*e.g.*, White and Dupré, 1986). Thus, crustal growth in an oceanic arc environment will produce TDM older than the time of crustal growth and initial

Table 2. Circa 1.4 Ga ages reported from metaigneous rocks of Oaxaquia.

Locality	Method	Comment	Age $\pm 2\sigma$	Reference
<i>Huiznopala Gneiss</i>				
<i>Mol9-4</i>	U-Pb LA-ICPMS	Upper intercept	1411 $\pm$ 27	This paper
<i>Mol9-5</i>	U-Pb LA-ICPMS	Upper intercept	1412 $\pm$ 59	This paper
Main series	Sm-Nd WR	12 point isochron	1403 $\pm$ 140	Lawlor <i>et al.</i> , 1999
<i>Guichicovi Complex</i>				
Metaigneous	Sm-Nd WR	16 point isochron	1435 $\pm$ 80	Weber & Köhler, 1999
<i>Oaxacan Complex</i>				
<i>Oax3-10-1</i>	U-Pb LA-ICPMS	Concordia age	1444 $\pm$ 16	This paper
El Catrín	U-Pb ID-TIMS	Upper intercept	1399 $\pm$ 58	Solari <i>et al.</i> , 2003
Pluma Hidalgo	U-Pb ID-TIMS	Upper intercept	1390 $\pm$ 45	Schulze, 2011
Pluma Hidalgo	U-Pb ID-TIMS	Upper intercept	1392 $\pm$ 91	Schulze, 2011

isotope ratios of Sm-Nd isochrons below the DM value. The Sm-Nd isochron ages instead correspond to the time of crust formation from such a mixed source.

In the view of the new U-Pb zircon ages presented here, an early Mesoproterozoic (~1.45 to ~1.40 Ga) igneous event is evident for the Main Series of the Huiznopala Gneiss and for the El Catrín migmatite of the northern Oaxacan Complex. There are two ways to explain ca. 1.4 Ga zircon in these rocks, whose igneous protoliths were previously

interpreted to be the result of arc magmatism ca. 1.2 byr ago: (model 1) the igneous protolith is ca. 1.4 Ga old with zircon ages representing the time of crust formation; followed by partial melting of this protolith at ca. 1.2 Ga or (model 2) inheritance from older continental crust assimilated into the ca. 1.2 Ga magmas.

*Early Mesoproterozoic crustal growth (model 1)*

Zircon from the 1411  $\pm$  27 Ma magmatic protolith of sample *Mol9-4*

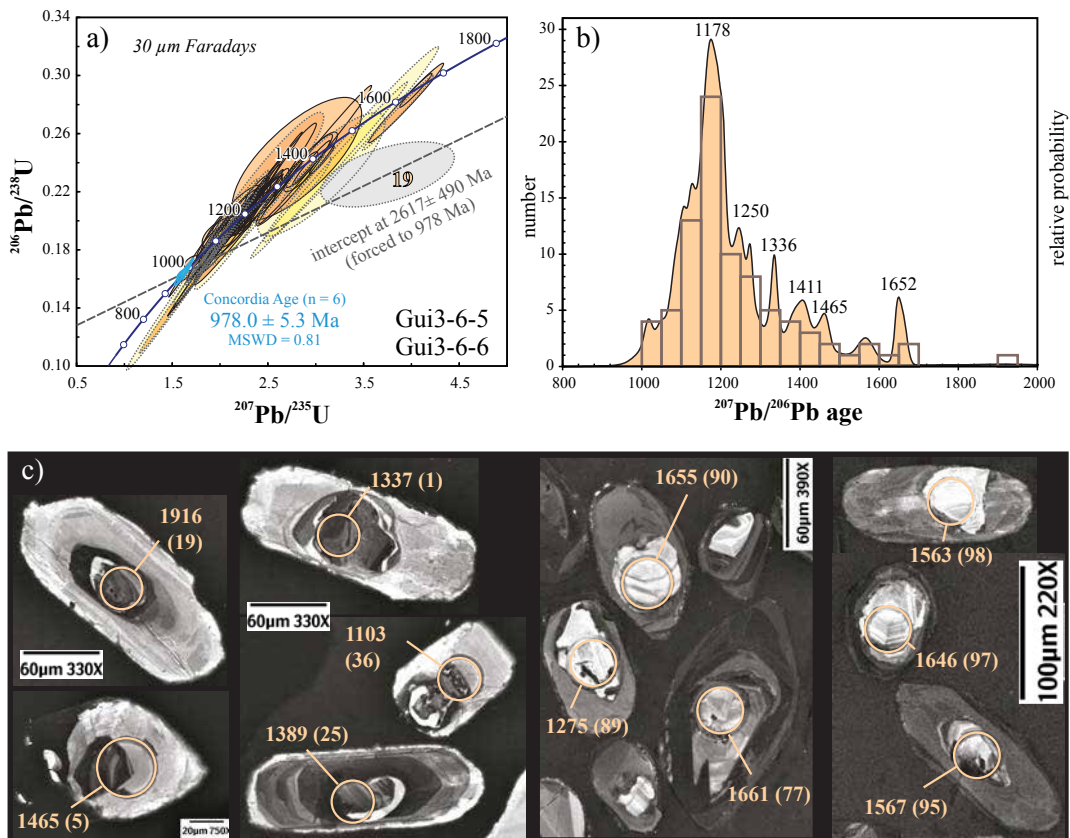


Figure 9. Zircon data of paragneiss samples from the Guichicovi Complex. (a) Concordia diagram of all analyzed zircons. Solid line error ellipses are concordant data, stippled lines ellipses are more than 5% discordant data. Spot 19 is a very old core with discordant isotope data and a discordia line forced to the age of metamorphism. (b) Histogram and relative probability plot of apparent  $^{207}\text{Pb}/^{206}\text{Pb}$  ages. Note: Blue error ellipses correspond to the age of metamorphism and the data are not included for provenance analyses. (c) CL images of typical zircon grains showing positions of spot analyses, apparent  $^{207}\text{Pb}/^{206}\text{Pb}$  ages, and (in parenthesis) analysis number from data table in Appendix 1 of the electronic supplement.

from the Main Series has initial Hf isotope ratios that plot on a 1.6 Ga  $TDM_{(Hf)}$  evolution line for a model crust with a  $^{177}Lu/^{176}Hf$  ratio of 0.015 (Figure 10). The initial Hf isotope compositions of *ca.* 1.2 Ga detrital zircon from the Huiznopala Supracrustal Unit and, within errors, also zircon from the gabbro-anorthosite (recalculated to 1.2 Ga protolith age) plots on the same crustal evolution line. This line connects with the fields of typical Oaxaquia arc zircon (Oaxacan Complex, Novillo Gneiss, and Guichicovi Complex) and of the  $\sim 1.04$ – $1.01$  Ga Pluma Hidalgo AMCG series (Figure 10; Weber *et al.*, 2010). These results are consistent with a model that explains the Oaxaquia arc terrane in terms of an oceanic island arc that evolved from a depleted mantle source in the early Mesoproterozoic (1.5 to 1.4 Ga). This mantle source was either less depleted than model mantle used for TDM ages (Vervoort *et al.*, 2000) or it was contaminated by subducted sediments. Since newly formed arc crust does not contain much differentiated magma, 1.4 Ga zircon is rare in Oaxaquia. Granitic arc magmatism occurred throughout Oaxaquia around 1.25 to 1.2 Ga. To generate the granitoids in such a model the Hf isotope alignment implies melting of the lower arc crust with only minor influence from the underlying mantle wedge. The Hf isotope data from zircons with typical Oaxaquia arc signature further indicate that zircon growth at any time between 1.2 and 1.0 Ga involved Hf with isotopic signature from the arc crust (with its corresponding radiogenic ingrowth) and not from inherited zircon (without significant radiogenic ingrowth).

#### *Inheritance from cratonic continental crust (model 2)*

Zircon data from the garnet-bearing charnockite *Mol9-5* from the same Main Series, suggest a contrasting scenario: the analyzed zircon grains have significantly lower Hf isotope ratios compared to *Mol9-4* and  $TDM_{(Hf)}$  model ages around 1.7 Ga, indicating an older crustal precursor. There is strong evidence for inheritance from older continental crust in this rock having zircon cores as old as  $\sim 1.7$  and  $>2.0$  Ga. The protolith crystallization age of  $1412 \pm 59$  Ma, however, is indistinguishable from those of sample *Mol9-4*. Interestingly, the  $^{177}Hf/^{176}Hf_{(1412Ma)}$  for three analyzed zircon grains are within errors identical, irrespective of the presence of an old  $\sim 1.7$  Ga core in one of these grains (see Figure 5h). The previously reported Hf isotope data from the Huiznopala Gneiss (Weber *et al.*, 2010) were obtained from zircon of a similar garnet-bearing orthogneiss. The initial  $^{177}Hf/^{176}Hf$  values are almost identical to those from sample *Mol9-5* (Figure 10) although ID-TIMS ages of these zircons are younger. With respect to the crustal evolution lines the latter zircons yield significantly older  $TDM_{(Hf)}$  ages, suggesting influence from another, older crust. But this is obviously not indicated in this case. It is instead likely that younger zircon recrystallized from previously existing zircon without adding external Hf to the crystal lattice (external Hf means from the crustal rock with its corresponding radiogenic ingrowth). Because zircon has extremely low  $^{177}Lu/^{176}Hf$  values ( $\sim 0.0005$ ) no significant radiogenic ingrowth occurs and, consequently, the  $^{177}Hf/^{176}Hf$  does not change by recrystallization whereas the radiogenic Pb of the U-Pb system is lost. The difference in zircon behavior might be explained by the protolith composition. It is likely that the precursor of the garnet-bearing charnockite was a peraluminous S-type granitoid magma in which only minor amount of zircon can be dissolved (Hoskin and Schaltegger, 2003). This S-type granite crystallized at  $1243 \pm 7$  Ma (Figure 7d) as indicated from igneous growth zones rimming  $\sim 1.4$  Ga and other, older cores. Consequently, continental crust older than typical Oaxaquia must have been present at the time when partial melting produced S-type magma. This implies that (1) Oaxaquia was already attached to the continent  $\sim 1.24$  byr ago or (2) sample *Mol9-5* is from a different unit that was emplaced during the later orogenic event (Zapotecan event; Solari *et al.*, 2003). However, protolith ages of

both analyzed samples are identical at  $\sim 1.41$  Ga and there are no field indications for a major thrust within the Main Series, which favors the first interpretation.

Mixing of older continental crust with typical Oaxaquia arc crust is evident from zircon of the El Catrín migmatite, which has significantly lower  $^{177}Hf/^{176}Hf$  in zircon with a *ca.* 1.4 Ga core compared to zircon that crystallized at *ca.* 1.25 Ga without inheritance. This difference cannot be explained by radiogenic ingrowth only, because it will require higher, mantle-like  $^{177}Lu/^{176}Hf$  values to produce the observed  $^{177}Hf/^{176}Hf$  at the given time difference. Therefore mixing is suggested to have occurred prior to the 1.25 Ga magmatism, which supports the abovementioned hypothesis that early Mesoproterozoic arc rocks were attached to the continent during the 1.25–1.2 Ga “Pluma Hidalgo” event (Schulze, 2011). Zircon cores from a different crustal precursor, which led to lower Hf isotope ratios in some zircons, were also reported from a migmatite of the southern Oaxacan Complex (Weber *et al.*, 2010; field marked with § in Figure 10).

#### **The provenance of metasedimentary rocks**

Surprisingly none of the 232 detrital zircon grains analyzed from the Huiznopala Supracrustal Unit reflects the time of the early Mesoproterozoic magmatic event of the nearby Main Series. Detrital zircons show intense oscillatory zoning without any inherited cores from older crust, suggesting provenance from granitoids that crystallized at *ca.* 1.25 to 1.2 Ga. The absence of early Mesoproterozoic detrital zircon suggests that (1) the older protoliths were not exposed at the time of sedimentation, (2) the early Mesoproterozoic Main Series is allochthonous with respect to the supracrustal rocks, or (3) the sample protoliths are of volcanosedimentary and not of clastic origin. The Hf isotope ratios of detrital zircon grains from the Huiznopala Supracrustal Unit plot close to a 1.6 Ga crustal evolution line for Hf, which is typical for Oaxaquia arc rocks (Figure 10). The  $\sim 1.4$  Ga zircons from sample *Mol9-4* plot on the same Hf evolution line suggesting a similar crustal source. Therefore it seems more likely that 1.5–1.4 Ga protoliths were not exposed to erosion during sediment deposition but, instead, they formed the crustal basement from which granitic magma was generated with the corresponding Hf isotope signature and these granites were later eroded.

The analyzed metasedimentary rocks from the Oaxacan Complex do not contain detrital zircon older than *ca.* 1.3 Ga, either. The major peaks are around 1.2 Ga and younger, subordinated peaks may be the result of ancient Pb-loss or recrystallization of zircon by a subsequent anatectic event as evidenced from the southern Oaxacan Complex (sample *Oax113011*). The maximum depositional age is difficult to constrain from the youngest detrital cores due to the abovementioned tectonothermal events. Significantly lower Hf isotope ratios (compared to typical Oaxaquia) of detrital zircons from paragneiss of the El Marquez structural unit (sample *Oax3-10-2*; Figure 10) imply provenance from a different, more evolved crust. Model ages ( $TDM_{(Hf)}$ ) in the range from 1.9 to 1.7 Ga for these detrital zircon grains are similar to those from the Garzón Massif of Colombia and from a charnockite of the Guichicovi Complex (Weber *et al.*, 2010). Although the ages of the detrital zircons are indistinguishable from those of paragneisses from the Huiznopala Supracrustal Unit and other metasedimentary rocks from the Oaxacan Complex (Solari *et al.*, 2012) their different Hf isotope compositions suggest tectonic emplacement of different crustal units during the Zapotecan event of the Grenville orogeny in México as proposed by Solari *et al.* (2003) on the basis of structural data and field relationships.

Clearly different and more continental sources are indicated from paragneiss zircons from the Guichicovi Complex, having early Mesoproterozoic, Paleoproterozoic, and probably even older zircon

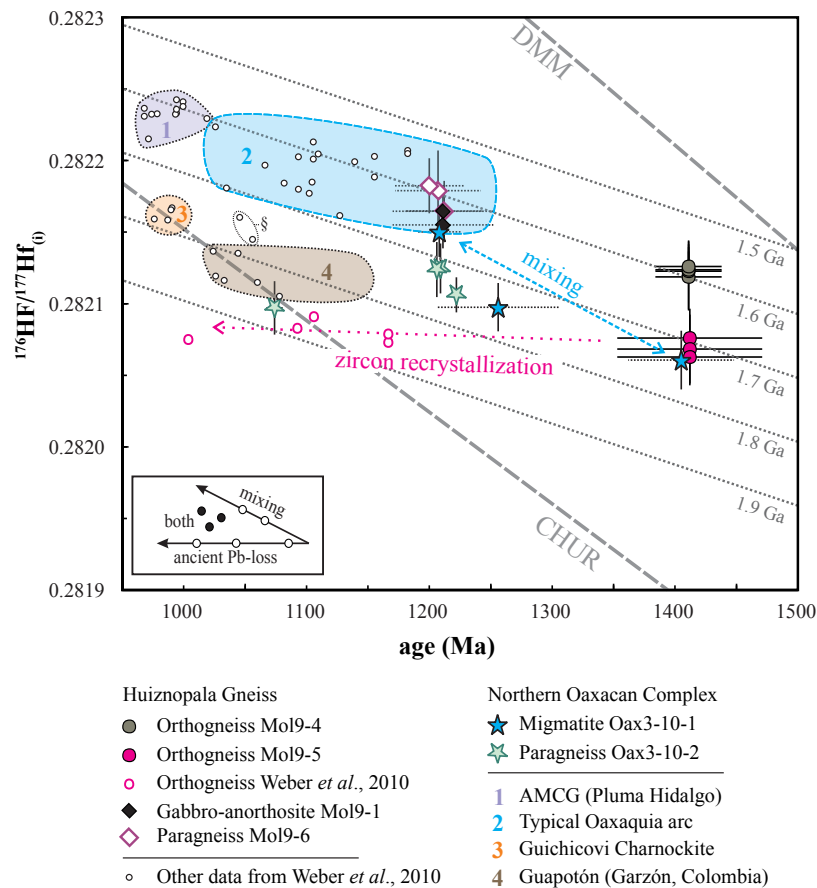


Figure 10.  $^{176}\text{Hf}/^{177}\text{Hf}$  vs time plot showing Hf isotope compositions of zircon grains from the Huiznopala Gneiss and the Oaxacan Complex (this work) compared with data from Weber *et al.* (2010). The  $^{176}\text{Hf}/^{177}\text{Hf}$  are recalculated to their  $^{207}\text{Pb}^*/^{206}\text{Pb}^*$  minimum crystallization ages (with stippled error bars if larger than symbols) except for zircon grains from orthogneiss samples *Mol9-4* and *Mol9-5* which are recalculated to their corresponding most reliable protolith igneous crystallization ages (solid error bars). Stippled grey lines illustrate Hf isotope evolution of crust separated from a depleted mantle at different times in Ga (crustal residence ages) with  $^{176}\text{Lu}/^{177}\text{Hf}$  of 0.015. Also shown are the evolution lines of CHUR (Bouvier *et al.*, 2008) and depleted model mantle (DMM; Vervoort *et al.*, 2000). - § = data of zircons with inherited pre-1.25 Ga zircon cores from the southern Oaxacan Complex.

cores. Most of the zircon cores from these metasediments have ages around 1.2 Ga, reinforcing the overwhelming importance of magmatism at this time. Besides that, older zircon cores are inherited in magmatic zircon crystallized at *ca.* 1.2 Ga. Abundant ~1.5 Ga detrital zircons together with ~1.2 and ~1.0 Ga zircon grains in early Paleozoic sedimentary rocks of the Maya Mountains in Belize (Martens *et al.*, 2010; Weber *et al.*, 2012), most of which having lower Hf isotope signatures compared to typical Oaxaquia zircons, suggest continental provenances. The new results from the Guichicovi Complex as part of the Maya block further suggest that the sources of the Paleozoic sediments might be continental sedimentary rocks that were emplaced on Oaxaquia at some point during the Grenville orogeny.

### Implications on the evolution and integrity of Oaxaquia

Based on evidence of orogenic activity and rifting from almost all earth's continental masses between 1.9 and 1.5 Ga a supercontinent named Columbia similar to Pangea was supposed (Figure 11a; *e.g.* Meert, 2012; Rogers and Santosh, 2002; Sears and Price, 2002). It is suggested that this supercontinent fragmented in early Mesoproterozoic times, leading to rift-related magmatism like mafic dyke swarms, AMCG suites, alkaline igneous provinces, and (Rapakivi-type) granite-rhyolite igneous provinces (Figure 11a). Within such a Columbia

realm, an early Mesoproterozoic arc established along the Laurentia, Amazonia and Baltica continental margins facing a "Pacific-like" Columbia ocean (Figure 11a; *e.g.* Rogers and Santosh, 2002). Oceanic magmatic arcs may have formed elsewhere in this ocean during and after Columbia fragmented and continental masses (like Baltica and Amazonia) started to drift and rotate. There is substantial evidence to suggest a "proto-Oaxaquia" oceanic arc with juvenile crust formation from 1.5 to 1.4 Ga. This hypothesis is constrained by whole-rock Sm-Nd isochrons (Lawlor *et al.*, 1999; Weber and Köhler, 1999) and U-Pb ages from zircon cores (Schulze, 2011; Solari *et al.*, 2003), and the igneous protolith ages of this work. A similar igneous protolith age is also reported from the Macarena uplift ( $1461 \pm 10$  Ma, Ibanez-Mejia *et al.*, 2011) in Colombia, which is either part of the autochthonous Putumaya Orogen underlying the Andean foreland southeast of the northwestern Andes (Ibanez-Mejia *et al.*, 2011) or the Macarena uplift is part of the northwestern Andes orogen that contains many discrete blocks of late Mesoproterozoic granulite terranes similar to Oaxaquia (Cardona *et al.*, 2010; Restrepo-Pace and Cediel, 2010; Restrepo-Pace *et al.*, 1997).

Geologic, paleomagnetic and age constrains suggest that Amazonia collided with (present day) eastern Laurentia along the Sunsas-Aguapei belts and the southern Appalachians, respectively, around 1.2 Ga and was then transported laterally along a sinistral megashear system

(Figures 11b, 11c; Tohver *et al.*, 2004, 2002). Subduction established at the leading edge of the Amazon craton as evidenced by widespread arc magmatism at this time elsewhere in the Northern Andes and Oaxaquia. Weber *et al.* (2010) proposed two active subduction zones, with an oceanic Oaxaquia arc and an active continental margin along Amazonia to explain differences between Hf isotope compositions of protoliths from the Garzón Massif of Colombia and those of typical Oaxaquia. Ibanez-Mejia *et al.* (2011) favor a single fringing arc system including all terranes having ~1.2 Ga arc magmatism and a back-arc basin, which separates sedimentary rocks that receive detritus only from the contemporaneous arc rocks and those deposited on a continental margin that also contain cratonic input.

The new data suggest that the proto-Oaxaquia arc terranes were probably attached to the Amazonia continental margin during *ca.* 1.25–1.2 Ga magmatic accretion, stitching together primitive arc protoliths with those from more evolved continental sources. Following the model of Tohver *et al.* (2004) who suggest Amazonia moving along Laurentia from present-day south to north after its collision with Laurentia 1.2 byr ago, the accretion of this fringing arc system to the (present day) northwestern margin of Amazonia can be explained (“Pluma Hidalgo” event by Schulze, 2011). Partial melting and formation of migmatites may have occurred along this continental margin within the same scenario at a later stage by ongoing compression at some time around 1.1 Ga during an Olmecan event as proposed by Solari *et al.* (2003). There is, however, no evidence for arc magmatism at this time in Oaxaquia.

**SUMMARY AND CONCLUSIONS**

Zircons from two orthogneiss samples of the Main Series from the Huiznopala Gneiss have igneous protolith ages of  $1411 \pm 27$  Ma and  $1412 \pm 59$  Ma. These igneous rocks are interpreted as represent-

ing the first expression of an early Mesoproterozoic “proto-Oaxaquia” magmatic arc. Typical 1.25 to 1.2 Ga Oaxaquia arc rocks evolved from a crustal precursor similar to a Main Series orthogneiss (*Mol9-4*). The initial Hf isotope ratios of zircon grains from this sample plot on a crustal evolution line that corresponds to a 1.6 Ga depleted mantle model age ( $TDM_{(Hf)}$ ). These results support a hypothesis that favors early Mesoproterozoic crust formation for Oaxaquia on the basis of Sm-Nd 1.5–1.4 Ga whole rock isochrons and  $TDM_{(Nd)}$  model ages (Lawlor *et al.*, 1999; Ruiz *et al.*, 1988; Weber and Köhler, 1999). Lower Hf isotope compositions of zircon from a garnet-bearing orthogneiss from the same unit, instead, indicate recycling of older rocks during ~1.4 Ga magmatism, suggesting the presence of continental crust basement, significantly different from typical Oaxaquia in this arc system.

Zircon cores from the El Catrin migmatite of the Oaxacan Complex also indicate an early Mesoproterozoic precursor ( $1.44 \pm 0.02$  Ga) with continental influence that was mixed with typical Oaxaquia rocks during the *ca.* 1.25–1.2 Ga arc magmatism. These results led to suggest that proto-Oaxaquia primitive arc was already attached to the active continental margin of Amazonia at this time and was then entirely intruded by magmatic arc granitic batholiths as indicated by 1.25 to 1.2 Ga igneous zircons elsewhere in Oaxaquia and in the northwestern Andes.

The absence of early Mesoproterozoic detrital zircon in paragneisses of the Huiznopala Gneiss and the Oaxacan Complex indicate that (1) sediments shed essentially from the 1.25 to 1.2 Ga igneous rocks or the samples correspond to contemporaneous volcanosedimentary layers and (2) that the early Mesoproterozoic rocks were not exposed or attached. Hafnium isotope signatures of detrital zircons from the Marquez paragneiss of the Oaxacan Complex differ from those of typical Oaxaquia, suggesting provenance from the continental margin. Paragneiss from the Guichicovi Complex also contains early Proterozoic detrital zircons indicating cratonic continental sources for part of the detritus.

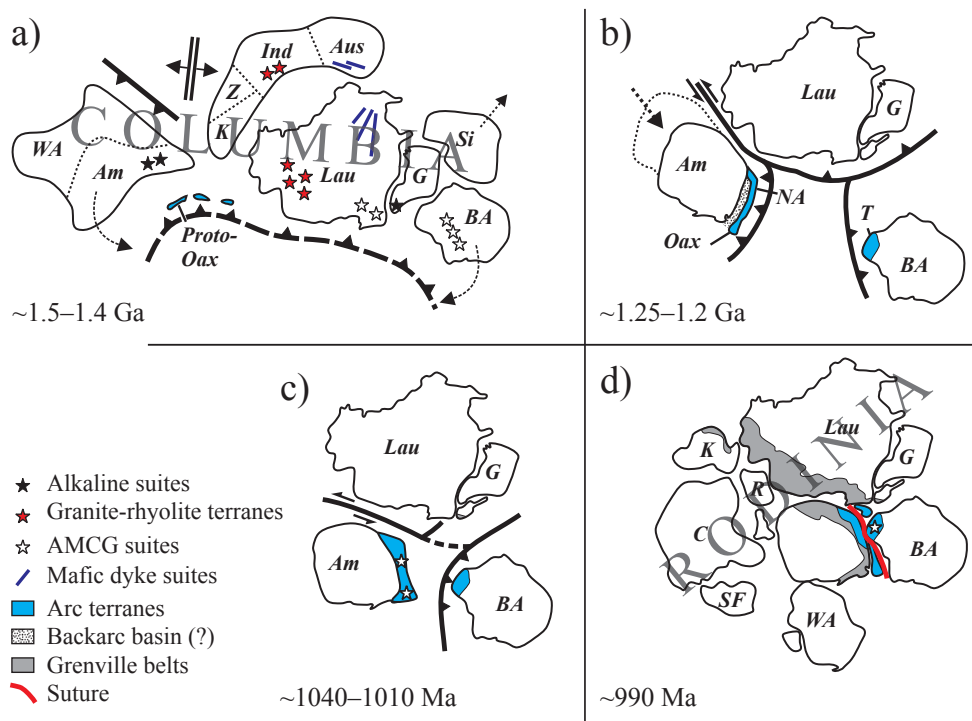


Figure 11. Paleogeographic model for the proto-Oaxaquia arc, Oaxaquia, and adjacent continental blocks illustrating the transition from Columbia to Rodinia supercontinents (modified from Ibanez-Mejia *et al.*, 2011; Li *et al.*, 2008; Rogers and Santosh, 2002; Weber *et al.*, 2010). For details see text. Abbreviations: Am = Amazonia, Aus = Australia, BA = Baltica-Sveconorwegia, C = Congo, G = Greenland, Ind = India, K = Kalahari, Lau = Laurentia, NA = Northern Andes, Oax = Oaxaquia, R = Rio de la Plata, SF = São Francisco, T = Telemarkia, WA = West Africa, Z = Zimbabwe.

## ACKNOWLEDGEMENTS

This contribution was supported by Consejo Nacional de Ciencia y Tecnología (CONACYT, Convocatoria Ciencia Básica 2007, project 79805). The authors wish to thank Mark E. Pecha for his help with data acquisition and reduction at Arizona LaserChron Center. We are grateful to George Gehrels and Joaquin Ruiz for providing access to the Arizona LaserChron Center, which is partially supported by a grant from the Instrumentation and Facilities Program, Division of Earth Sciences, NSF-EAR 0732436. Special thanks go to Erik E. Scherer, University of Münster, for his help with running the Isoprobe and reducing the Lu-Hf data. Thanks go to Rogelio Sosa-Valdes, Susana Rosas-Montoya, Victor Pérez-Arroyoz, and Gabriel Rendón-Márquez (all CICESE) for their help with sample preparation and zircon separation. Thanks go also to Mariela Carrera-Muñoz (CICESE) for running the clean lab and to Luis Gradilla-Martínez (CICESE) for performing CL images. Special thanks go to Henry Coombs (University of Cardiff) for reviewing the manuscript, to the reviewers Uwe Martens (Tectonic Analyses Inc.) and Fernando Ortega (UNAM) for their helpful and constructive comments, and to editor Peter Schaaf (UNAM) for his final revision.

## REFERENCES

- Arndt, N.T., Goldstein, S.L., 1987, Use and abuse of crust-formation ages: *Geology* 15, 893-895.
- Bizzarro, M., Baker, J.A., Haack, H., Ulfbeck, D., Rosing, M., 2003, Early history of Earth's crust-mantle system inferred from hafnium isotopes in chondrites: *Nature* 421, 931-933.
- Blichert-Toft, J., Boyet, M., Télouk, P., Albarède, F., 2002,  $^{147}\text{Sm}$ - $^{143}\text{Nd}$  and  $^{176}\text{Lu}$ - $^{176}\text{Hf}$  in eucrites and the differentiation of the HED parent body: *Earth and Planetary Science Letters*, 204, 167-181.
- Bouvier, A., Vervoort, J.D., Patchett, P.J., 2008, The Lu-Hf and Sm-Nd isotopic composition of CHUR: Constraints from unequilibrated chondrites and implications for the bulk composition of terrestrial planets. *Earth Planet. Sci. Lett.* 273, 48-57.
- Cameron, K.L., Lopez, R., Ortega-Gutiérrez, F., Solari, L.A., Keppie, J.D., Schulze, C., 2004, U-Pb geochronology and Pb isotopic compositions of leached feldspars: Constraints on the origin and evolution of Grenville rocks from eastern and southern Mexico: *Geological Society of America, Memoirs* 197, 755-769.
- Cardona, A., Chew, D., Valencia, V.A., Bayona, G., Mišković, A., Ibanez-Mejía, M., 2010, Grenvillian remnants in the Northern Andes: Rodinian and Phanerozoic paleogeographic perspectives: *Journal of South American Earth Sciences*, 29, 92-104.
- Condie, K.C., Beyer, E., Belousova, E., Griffin, W.L., O'Reilly, S.Y., 2005, U-Pb isotopic ages and Hf isotopic composition of single zircons: The search for juvenile Precambrian continental crust: *Precambrian Research* 139, 42-100.
- Cruz-Urbe, A.M., Feineman, M.D., Zack, T., Barth, M., 2014, Metamorphic reaction rates at 650–800 °C from diffusion of niobium in rutile: *Geochimica et Cosmochimica Acta*, 130, 63-77.
- DePaolo, D., 1981, Neodymium isotopes in the Colorado Front Range and crust-mantle evolution in the Proterozoic: *Nature* 291, 193-196.
- Fries, C.J., 1962a, Reseña de los métodos principales empleados en las determinaciones isotópicas de edad: Universidad Nacional Autónoma de México, Instituto de Geología, Boletín 64, 1-9.
- Fries, C.J., 1962b, Lista de fechas geoquímicas reportadas para minerales y rocas mexicanas, con un comentario sobre su significado geológico y geotectónico, Universidad Nacional Autónoma de México, Instituto de Geología, Boletín, 64, 85-109.
- Fries, C.J., Rincón-Orta, C., 1965, Nuevas aportaciones geocronológicas y técnicas empleadas en el laboratorio de geocronometría: Universidad Nacional Autónoma de México, Instituto de Geología, Boletín 73, 57-133.
- Fries, C.J., Schmitter, E., 1962, Rocas precámbricas de edad Grenvilliana en la parte central de Oaxaca en el sur de México: Universidad Nacional Autónoma de México, Instituto de Geología, Boletín, 64, 45-53.
- Fries, C.J., Schlaepfer, C.J., Rincón-Orta, C., 1966, Nuevos datos geocronológicos del Complejo Oaxaqueño: Boletín de la Sociedad Geológica Mexicana 29, 59-66.
- Gehrels, G.E., Valencia, V.A., Ruiz, J., 2008, Enhanced precision, accuracy, efficiency, and spatial resolution of U-Pb ages by laser ablation-multicollector-inductively coupled plasma-mass spectrometry: *Geochemistry, Geophysics, Geosystems*, 9.
- Hoskin, P.W.O., Schaltegger, U., 2003, The Composition of Zircon and Igneous and Metamorphic Petrogenesis: Reviews in Mineralogy and Geochemistry, 53, 27-62.
- Ibanez-Mejía, M., Ruiz, J., Valencia, V.A., Cardona, A., Gehrels, G.E., Mora, A.R., 2011, The Putumayo Orogen of Amazonia and its implications for Rodinia reconstructions: New U-Pb geochronological insights into the Proterozoic tectonic evolution of northwestern South America: *Precambrian Research*, 191, 58-77.
- Johnston, S., Gehrels, G., Valencia, V., Ruiz, J., 2009, Small-volume U-Pb zircon geochronology by laser ablation-multicollector-ICP-MS: *Chemical Geology*, 259, 218-229.
- Keppie, J.D., 2004, Terranes of Mexico revisited: A 1.3 billion year odyssey: *International Geology Review*, 46, 765-794.
- Keppie, J.D., Ortega-Gutiérrez, F., 2010, 1.3 - 0.9 Ga Oaxaquia (Mexico): Remnant of an arc/backarc on the northern margin of Amazonia: *Journal of South American Earth Sciences*, 29, 21-27.
- Keppie, J.D., Dostal, J., Ortega-Gutiérrez, F., Lopez, R., 2001, A Grenvillian arc on the margin of Amazonia: evidence from the southern Oaxacan Complex, southern Mexico: *Precambrian Research*, 112, 165-181.
- Keppie, J.D., Dostal, J., Cameron, K.L., Solari, L.A., Ortega-Gutiérrez, F., Lopez, R., 2003, Geochronology and geochemistry of Grenvillian igneous suites in the northern Oaxacan Complex, southern Mexico: tectonic implications: *Precambrian Research*, 120, 365-389.
- Keppie, J.D., Solari, L.A., Ortega-Gutiérrez, F., Ortega-Rivera, A., Lee, J.K.W., Lopez, R., Hames, W.E., 2004, U-Pb and  $^{40}\text{Ar}/^{39}\text{Ar}$  constraints on the cooling history of the northern Oaxacan Complex, southern Mexico: Tectonic implications: *Geological Society of America, Memoirs*, 197, 771-781.
- Kuegelgen, H.V., 1958, Der Aufbau der zentralen Sierra Madre Oriental, Mexico: *Zeitschrift der Deutschen Geologischen Gesellschaft Band* 110, 117-142.
- Lawlor, P.J., Ortega-Gutiérrez, F., Cameron, K.L., Ochoa-Camarillo, H., Lopez, R., Sampson, D.E., 1999, U-Pb geochronology, geochemistry, and provenance of the Grenvillian Huiznopala Gneiss of Eastern Mexico: *Precambrian Research*, 94, 73-99.
- Lee, J.K.W., Williams, I.S., Ellis, D.J., 1997, Pb, U and Th diffusion in natural zircon: *Nature* 390, 159-162.
- Li, Z.X., Bogdanova, S.V., Collins, A.S., Davidson, A., De Waele, B., Ernst, R.E., Fitzsimons, I.C.W., Fuck, R.A., Gladkochub, D.P., Jacobs, J., Karlstrom, K.E., Lu, S., Natapov, L.M., Pease, V., Pisarevsky, S.A., Thrane, K., Vernikovsky, V., 2008, Assembly, configuration, and break-up history of Rodinia: A synthesis: *Precambrian Research*, 160, 179-210.
- Ludwig, K.R., 2008, *Isoplot 3.60*: Berkeley Geochronology Center Special Publication, 4, 77.
- Ludwig, K.R., Mundil, R., 2002, Extracting reliable U-Pb ages and errors from complex populations of zircons from Phanerozoic tuffs: *Geochimica et Cosmochimica Acta*, 66, A463.
- Martens, U., Weber, B., Valencia, V.A., 2010, U/Pb geochronology of Devonian and older Paleozoic beds in the southeastern Maya block, Central America: Its affinity with peri-Gondwanan terranes: *Geological Society of America Bulletin*, 122, 815-829.
- Meert, J.G., 2012, What's in a name? The Columbia (Paleopangaea/Nuna) supercontinent: *Gondwana Research*, 21, 987-993.
- Möller, A., O'Brien, P.J., Kennedy, A., Kröner, A., 2002, Polyphase zircon in ultrahigh-temperature granulites (Rogaland, SW Norway): constraints for Pb diffusion in zircon: *Journal of Metamorphic Geology*, 20, 727-740.
- Murillo-Muñeton, G., 1994, Petrologic and geochronologic study of Grenville-age granulites and post-granulite plutons from the La Mixtequita area, state of Oaxaca in southern Mexico, and their tectonic significance: Los Angeles, Cal., USA, University of Southern California, master thesis, 163 pp.
- Nebel-Jacobsen, Y., Scherer, E.E., Münker, C., Mezger, K., 2005, Separation

- of U, Pb, Lu, and Hf from single zircons for combined U–Pb dating and Hf isotope measurements by TIMS and MC-ICPMS: *Chemical Geology*, 220, 105-120.
- Ochoa-Camarillo, H., 1996, *Geología del Anticlinorio de Huayacocotla en la Región de Molango, Estado de Hidalgo, México*: Universidad Autónoma Nacional de México, México, master thesis, 91 pp.
- Ortega-Gutiérrez, F., Mitre-Salazar, L.M., Morán-Centeno, D. J., Alaniz-Álvarez, S.A., Nieto-Samaniego, Á.F., 1992, *Carta geológica de la República Mexicana, escala 1:2,000,000*: Universidad Nacional Autónoma de México, Instituto de Geología.
- Ortega-Gutiérrez, F., Ruiz, J., Centeno-García, E., 1995, Oaxaquia, a Proterozoic microcontinent accreted to North America during the late Paleozoic: *Geology* 23, 1127-1130.
- Patchett, P.J., Ruiz, J., 1987, Nd isotopic ages of crust formation and metamorphism in the Precambrian of eastern and southern Mexico: *Contributions to Mineralogy and Petrology*, 96, 523-528.
- Restrepo-Pace, P.A., Cedié, F., 2010, Northern South America basement tectonics and implications for paleocontinental reconstructions of the Americas: *Journal of South American Earth Sciences*, 29, 764-771.
- Restrepo-Pace, P.A., Ruiz, J., Gehrels, G., Cosca, M., 1997, Geochronology and Nd isotopic data of Grenville-age rocks in the Colombian Andes: new constraints for Late Proterozoic-Early Paleozoic paleocontinental reconstructions of the Americas. *Earth and Planetary Science Letters*, 150, 427-441.
- Rogers, J.J.W., Santosh, M., 2002, Configuration of Columbia, a Mesoproterozoic Supercontinent: *Gondwana Research*, 5, 5-22.
- Ruiz, J., Patchett, P.J., Ortega-Gutiérrez, F., 1988, Proterozoic and Phanerozoic basement terranes of Mexico from Nd isotopic studies: *Geological Society of America Bulletin* 100, 274-281.
- Ruiz, J., Tosdal, R.M., Restrepo, P.A., Murillo-Muñetón, G., 1999, Pb isotope evidence for Colombia-southern México connections in the Proterozoic: *Geological Society of America Special Paper*, 336, 183-197.
- Scherer, E., Cameron, K.L., Blichert-Toft, J., 2000, Lu–Hf garnet geochronology: Closure temperature relative to the Sm–Nd system and the effects of trace mineral inclusions: *Geochimica et Cosmochimica Acta*, 64, 3413-3432.
- Scherer, E., Munker, C., Mezger, K., 2001, Calibration of the Lutetium–Hafnium Clock: *Science* 293, 683-687.
- Schulze, C., 2011, *Petrología y geoquímica de las rocas del área de Pluma Hidalgo, Oaxaca e implicaciones tectónicas para el Proterozoico de Oaxaquia*: Universidad Autónoma Nacional de México, México, PhD thesis, 311 pp.
- Sears, J.W., Price, R.A., 2002, The Hypothetical Mesoproterozoic Supercontinent Columbia: Implications of the Siberian–West Laurentian Connection: *Gondwana Research*, 5, 35-39.
- Söderlund, U., Patchett, P.J., Vervoort, J.D., Isachsen, C.E., 2004, The 176Lu decay constant determined by Lu–Hf and U–Pb isotope systematics of Precambrian mafic intrusions: *Earth and Planetary Science Letters* 219, 311-324.
- Solari, L.A., Keppie, J.D., Ortega-Gutiérrez, F., Cameron, K., Lopez, R., Hames, W., 2003, 990 and 1100 Ma Grenvillian tectonothermal events in the northern Oaxacan complex, southern México: roots of an orogen: *Tectonophysics* 365, 257-282.
- Solari, L.A., Keppie, J.D., Ortega-Gutiérrez, F., Cameron, K.L., Lopez, R., 2004, ~990 Ma peak granulitic metamorphism and amalgamation of Oaxaquia, Mexico: U – Pb zircon geochronological and common Pb isotopic data 212-225.
- Solari, L.A., Ortega-Gutiérrez, F., Ortega-Obregón, C., Macías-Romo, C., Reyes-Salas, M., 2012, Detrital provenance of the Grenvillian Oaxacan Complex, Southern Mexico: a zircon perspective: *Geological Society of America, Abstracts with Programs*, 44, 4.
- Stacey, J.S., Kramers, J.D., 1975, Approximation of terrestrial lead isotope evolution by a two-stage model: *Earth and Planetary Science Letters*, 26, 207-221.
- Tohver, E., van der Pluijm, B. a., Van der Voo, R., Rizzotto, G., Scandolaro, J.E., 2002, Paleogeography of the Amazon craton at 1.2 Ga: early Grenvillian collision with the Llano segment of Laurentia: *Earth and Planetary Science Letters*, 199, 185-200.
- Tohver, E., Bettencourt, J.S., Tosdal, R., Mezger, K., Leite, W.B., Payolla, B.L., 2004, Terrane transfer during the Grenville orogeny: tracing the Amazonian ancestry of southern Appalachian basement through Pb and Nd isotopes: *Earth and Planetary Science Letters*, 228, 161-176.
- Vervoort, J.D., Patchett, P.J., Albarède, F., Blichert-Toft, J., Rudnick, R., Downes, H., 2000, Hf–Nd isotopic evolution of the lower crust: *Earth and Planetary Science Letters*, 181, 115-129.
- Weber, B., Hecht, L., 2003, Petrology and geochemistry of metaigneous rocks from a Grenvillian basement fragment in the Maya block: the Guichicovi Complex, Oaxaca, southern Mexico: *Precambrian Research*, 124, 41-67.
- Weber, B., Köhler, H., 1999, Sm–Nd, Rb–Sr and U–Pb geochronology of a Grenville Terrane in Southern Mexico: origin and geologic history of the Guichicovi Complex: *Precambrian Research*, 96, 245-262.
- Weber, B., Scherer, E.E., Schulze, C., Valencia, V.A., Montecinos, P., Mezger, K., Ruiz, J., 2010, U–Pb and Lu–Hf isotope systematics of lower crust from central-southern Mexico – Geodynamic significance of Oaxaquia in a Rodinia Realm: *Precambrian Research*, 182, 149-162.
- Weber, B., Scherer, E.E., Martens, U.K., Mezger, K., 2012, Where did the lower Paleozoic rocks of Yucatan come from? A U–Pb, Lu–Hf, and Sm–Nd isotope study: *Chemical Geology*, 312-313, 1-17.
- White, W.M., Dupré, B., 1986, Sediment subduction and magma genesis in the Lesser Antilles: Isotopic and trace element constraints: *Journal of Geophysical Research: Solid Earth*, 91, 5927-5941.

Manuscript received: September 3, 2013

Corrected manuscript received: March 25, 2014

Manuscript accepted: April 23, 2014